



Mouse Tumor-Bearing Models as Preclinical Study Platforms for Oral Squamous Cell Carcinoma

Qiang Li^{1†}, Heng Dong^{1,2†}, Guangwen Yang¹, Yuxian Song¹, Yongbin Mou^{1,2*} and Yanhong Ni^{1*}

¹ Central Laboratory, Nanjing Stomatological Hospital, Medical School of Nanjing University, Nanjing, China, ² Department of Oral Implantology, Nanjing Stomatological Hospital, Medical School of Nanjing University, Nanjing, China

OPEN ACCESS

Edited by:

Christian Simon,
Lausanne University Hospital
(CHUV), Switzerland

Reviewed by:

Ruud Brakenhoff,
VU University Medical
Center, Netherlands
Vincent Roh,
Lausanne University Hospital
(CHUV), Switzerland

*Correspondence:

Yongbin Mou
yongbinmou@163.com
Yanhong Ni
niyanhong12@163.com

[†]These authors have contributed
equally to this work

Specialty section:

This article was submitted to
Head and Neck Cancer,
a section of the journal
Frontiers in Oncology

Received: 23 September 2019

Accepted: 06 February 2020

Published: 25 February 2020

Citation:

Li Q, Dong H, Yang G, Song Y, Mou Y
and Ni Y (2020) Mouse Tumor-Bearing
Models as Preclinical Study Platforms
for Oral Squamous Cell Carcinoma.
Front. Oncol. 10:212.
doi: 10.3389/fonc.2020.00212

Preclinical animal models of oral squamous cell carcinoma (OSCC) have been extensively studied in recent years. Investigating the pathogenesis and potential therapeutic strategies of OSCC is required to further progress in this field, and a suitable research animal model that reflects the intricacies of cancer biology is crucial. Of the animal models established for the study of cancers, mouse tumor-bearing models are among the most popular and widely deployed for their high fertility, low cost, and molecular and physiological similarity to humans, as well as the ease of rearing experimental mice. Currently, the different methods of establishing OSCC mouse models can be divided into three categories: chemical carcinogen-induced, transplanted and genetically engineered mouse models. Each of these methods has unique advantages and limitations, and the appropriate application of these techniques in OSCC research deserves our attention. Therefore, this review comprehensively investigates and summarizes the tumorigenesis mechanisms, characteristics, establishment methods, and current applications of OSCC mouse models in published papers. The objective of this review is to provide foundations and considerations for choosing suitable model establishment methods to study the relevant pathogenesis, early diagnosis, and clinical treatment of OSCC.

Keywords: mouse models, OSCC, chemical carcinogen-induced, transplanted, xenograft, syngeneic, HPV, genetically engineered models

INTRODUCTION

Oral squamous cell carcinoma (OSCC) is one of the most common human malignancies and endangers human health, and it accounts for 40% of all head and neck squamous cell carcinoma (HNSCC) cases (1, 2). Although cancer treatments have developed rapidly, the 5-year survival rate for OSCC is still only remained at 50% over the last few decades (3–5). Given the high incidence and poor prognosis of OSCC, an increasing number of researchers are conducting in-depth investigations into the pathogenesis and potential therapeutic targets of OSCC (6–10).

Researches on OSCC can be performed both *in vitro* and *in vivo*. Although experiments *in vitro* have the advantages of relative simplicity, species specificity, convenience, and automation, the extrapolation of *in vitro* results to predict the behavior of tumors in intact organisms is challenging (11). By contrast, experiments *in vivo* using animal models are representative of whole organisms and the use of animal models can avoid issues related to safety, ethics, and extended research cycles that arise in human experiments. Moreover, animal models can accurately reflect the tumor

microenvironment—which includes a variety of cytokines, infiltrating immune cells, tumor stroma, and blood vessels—and significant tumor biological behaviors, such as invasion and metastasis. Therefore, a suitable animal model is a prerequisite for clarifying the initiation and progression of OSCC.

Previous researches have revealed that several kinds of animals can be used to establish OSCC models, including hamsters, rats, mice, dogs, and cats (12–17). As early as 1954, squamous cell carcinoma (SCC) of the cheek was induced in hamsters by 9,10-dimethyl-1,2-benzanthracene (DMBA), and hamster SCC exhibits many similarities to human OSCC, including the morphology, histology, infiltration and metastasis, expression of biomarkers, and genetic and epigenetic alterations (18–24). Nevertheless, this model also has its shortcomings, for example, the humans lack cheek pouches, and hamster cheek pouches have inadequate lymphatic drainage (25). Moreover, non-murine models have also been used for the research of OSCC etiology, treatment, and tumor-immune system interactions (17). For example, the metastasis and bone invasion of OSCC has been studied in cats, which can be used to mimic highly malignant OSCC (16, 26, 27), and OSCC has also been researched using dogs for identifying risk factors associated with survival in dogs with non-tonsillar OSCC (15). However, there are fewer reagents available to study dogs and cats, and species-specific drug metabolism and solubility issues are challenging to solve with these models (28).

Rodents other than hamsters, especially rats and mice, are the most commonly used animals in OSCC modeling. The rats are larger but correspondingly more expensive, and there are few immunodeficient or genetically engineered rats. The mouse is characterized by small size, a propensity to breed in captivity, a lifespan of 3 years, extensive physiological and molecular similarities to humans, and an entirely sequenced genome (29). The abundance of particular types of mice, such as immunodeficient mice, genetically engineered mice, and humanized mice, provides a variety of new platforms for the establishment of OSCC models. Therefore, OSCC mouse models have attracted increasing attention from numerous scholars in the OSCC research field.

This review focuses on several aspects of OSCC mouse models and is organized by the three main methods by which these models are established: chemical carcinogen-induced, transplanted, and genetically modified OSCC mouse models (Figure 1). Details are provided on the selection and establishment of OSCC mouse models and differences in their mechanisms, characteristics, establishment methods, and applications. This review aims to provide a reference and direction for researchers who are working toward conquering OSCC.

CHEMICAL CARCINOGEN-INDUCED MOUSE MODELS

The main risk factors for OSCC include tobacco, alcohol, long-term chewing of betel quid, human papillomavirus (HPV), and oral lichen planus (especially the erosive form) (30, 31). There are

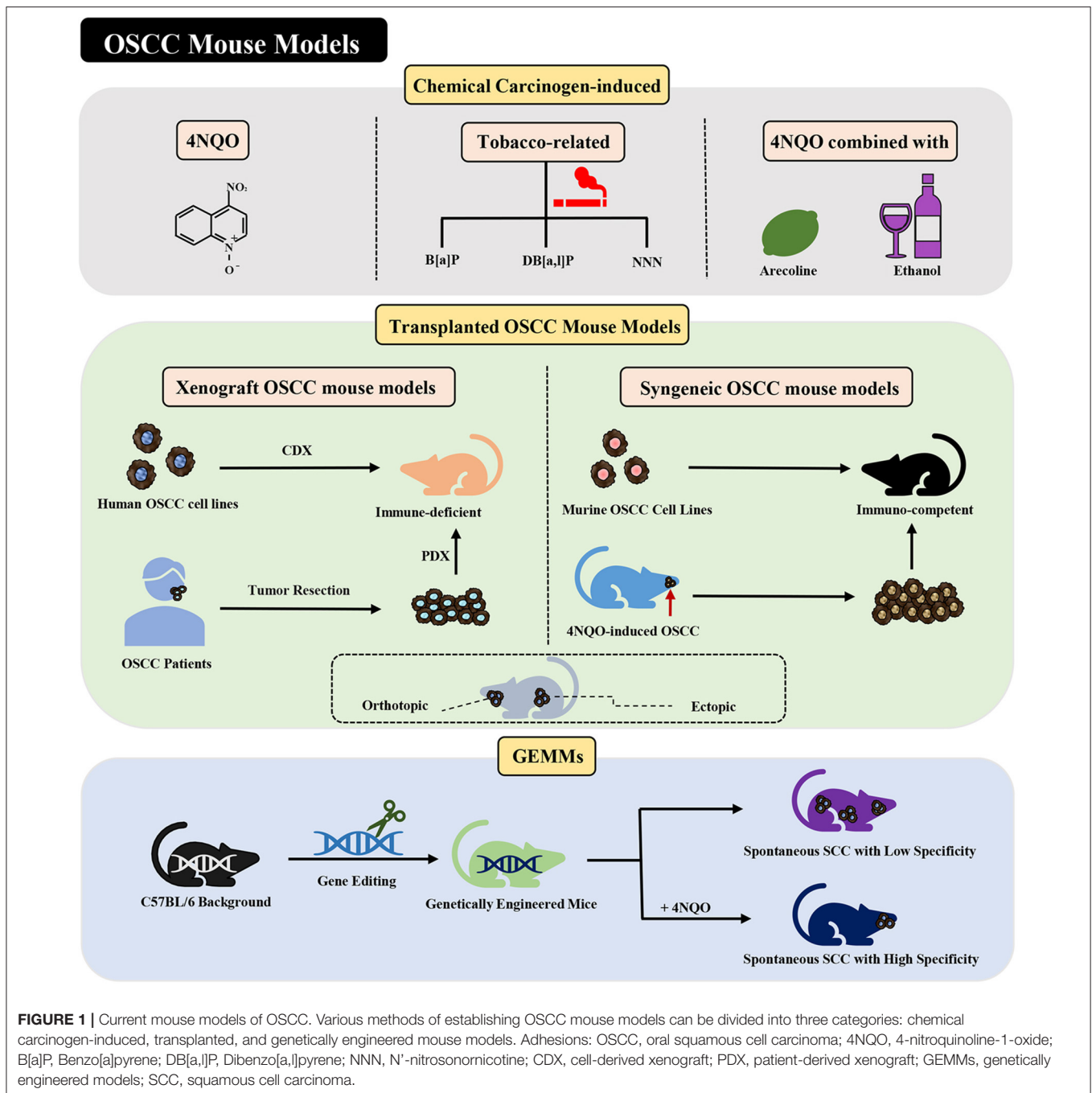
more than 60 carcinogens in cigarette smoke and 16 in unburned tobacco, including tobacco-specific nitrosamines [such as 4-(methylnitrosamino)-1-(3-pyridyl)-1-butanone (NNK) and N'-nitrosonornicotine (NNN)], polycyclic aromatic hydrocarbons (PAHs, such as benzo[a]pyrene), and aromatic amines (such as 4-aminobiphenyl) (32). These chemicals have been reported to induce DNA adducts and correlate with a predisposition to cancer. DNA adducts—the result of covalent binding between DNA and carcinogens, related substances, or their metabolites—are central in the carcinogenesis caused by these agents (32, 33).

Knowing the above-mentioned risk factors for OSCC, researchers have induced murine oral carcinogenesis using a variety of chemical carcinogens, such as 4-nitroquinoline-1-oxide (4NQO) (34), Benzo[a]pyrene (B[a]P) (35), Dibenzo[a,l]pyrene (DB[a,l]P) (36, 37), NNN (37), and combination of 4NQO and arecoline or ethanol (38, 39). The exposure of these chemical carcinogens to the oral cavity of mice can naturally produce a primary OSCC mouse model.

4NQO-Induced OSCC Mouse Model

Mechanism of 4NQO-Induced OSCC Mouse Model

The compound 4NQO is an aromatic amine heterocyclic compound and a precursor carcinogen that is typically manufactured for research purposes. Currently, it is the most recognized and frequently used chemical carcinogen for establishing chemical carcinogen-induced OSCC mouse models (40). Researches have proved that 4NQO mimics tobacco and plays a carcinogenic role by causing intracellular oxidative stress, DNA adduction, mutagenesis, and tumor induction (Figure 2) (41–43). It has been revealed as a potent inducer of intracellular oxidative stress by generating reactive oxygen species (ROS) (44, 45), which is related to carcinogenesis that is caused by DNA damage (46–49). Although 4NQO is not a direct carcinogen, it is an electrophilic species produced by metabolism in the body and undergoes an irreversible reaction with the nucleophilic part of DNA, which ultimately introduce mutations. The carcinogenic action of 4NQO is initiated by the enzymatic reduction of its nitro group: first, 4NQO is reduced to 4-hydroxy amino quinoline-1-oxide (4HAQO) by NADH and NAD(P)H, which thus act as 4NQO nitroreductase and quinone reductase, respectively (50). Then, 4HAQO can be acetylated by seryl-tRNA synthetase to form a seryl-AMP enzyme complex (51). The resultant 4HAQO and seryl-AMP enzyme complex are carcinogenic metabolites that induce the formation of DNA adducts. The cellular detoxification of 4NQO is carried out by multidrug resistance protein (MRP) and glutathione S-transferase P (GSTP1-1), which may play essential roles in preventing the initiation and progression events of carcinogenesis (52). The imbalance between the two pathways is the leading cause of tumor induction by 4NQO. Nuclear magnetic resonance (NMR) studies and *in vivo* experiments have revealed that 4HAQO binds preferentially to G residues of DNA (53, 54). Moreover, the third and fourth position of the acetylated metabolite of 4NQO can react with the N2 and C8 positions of guanine (55). Mutations caused by these DNA adducts result in guanine to pyrimidine substitution (56, 57).



Characteristics of the 4NQO-Induced OSCC Mouse Model

The 4NQO-induced mouse model reflects the multistage dynamic carcinogenicity of human OSCC, from dysplasia to invasion. Researchers using this model reported that the gross morphology of lesions changed from mild to severe dysplasia (Figure 3A), and the pathological stages of tongue lesions underwent hyperplasia, dysplasia (mild, moderate, and severe), *in situ* carcinoma, and invasive squamous cell carcinoma (SCC) (Figure 3B) (58). One of the characteristics of this model is

that not all mice develop the same lesions at the same time, and a variety of lesions can be seen on the tongue of a single mouse (Figure 3C). In a study using the 4NQO-induced oral cancer pain model, adult female C57BL/6 mice were given 4NQO (100 µg/mL) dissolved in propylene glycol for 16 weeks. The treatment was then switched to regular drinking water for 16–28 weeks. By 28 weeks, pathological changes in the tongue were observed in all mice, of which 20.8% had moderate atypical hyperplasia, 45.9% developed severe atypical hyperplasia and carcinoma *in situ*, and 33.3% progressed to squamous cell

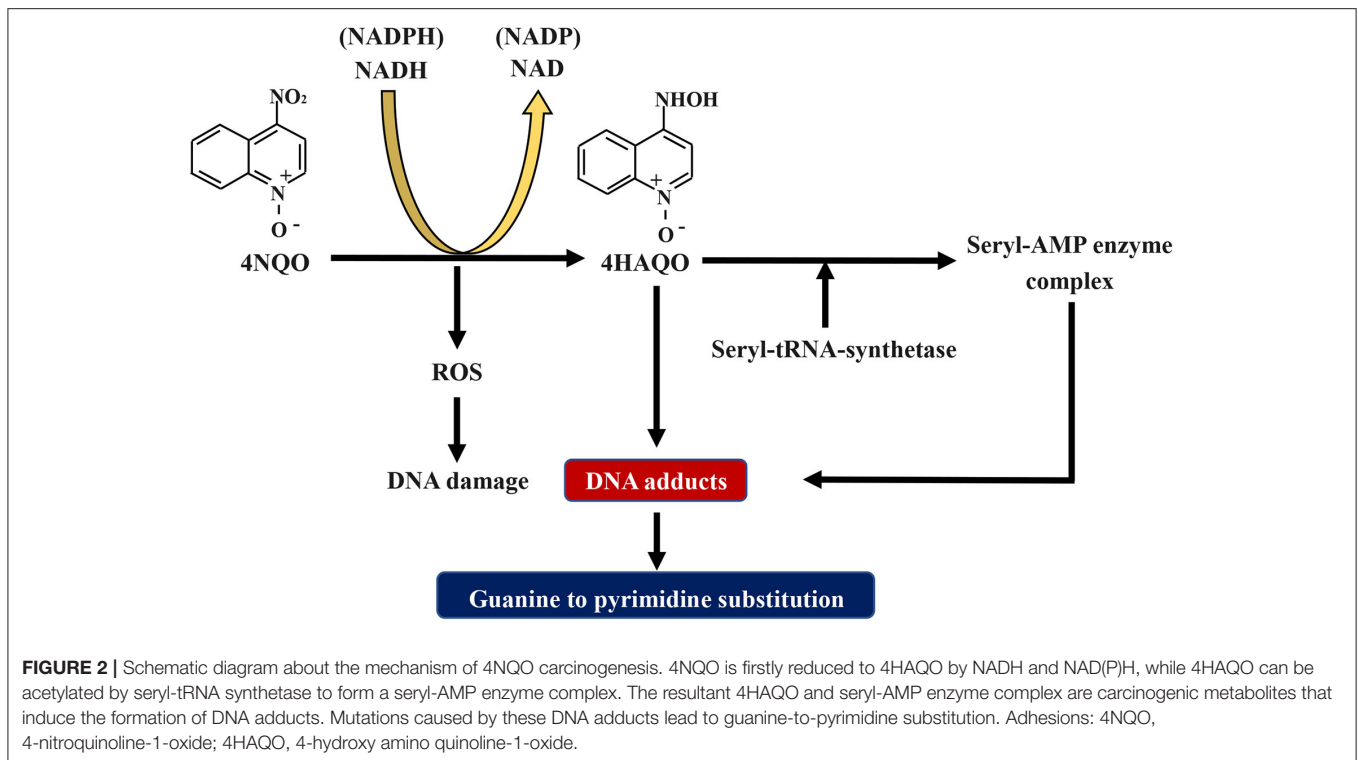


FIGURE 2 | Schematic diagram about the mechanism of 4NQO carcinogenesis. 4NQO is firstly reduced to 4HAQO by NADH and NAD(P)H, while 4HAQO can be acetylated by seryl-tRNA synthetase to form a seryl-AMP enzyme complex. The resultant 4HAQO and seryl-AMP enzyme complex are carcinogenic metabolites that induce the formation of DNA adducts. Mutations caused by these DNA adducts lead to guanine-to-pyrimidine substitution. Adhesions: 4NQO, 4-nitroquinoline-1-oxide; 4HAQO, 4-hydroxy amino quinoline-1-oxide.

carcinoma (61). But the OSCC mouse model established by this method had a low degree of malignancy and rarely underwent metastasis and bone invasion (40).

The molecular events showing in the 4NQO-induced mouse model closely resemble those observed in human HNSCC patients (62, 63). Moreover, the 4NQO-induced OSCC mouse model has been proved effective because it is very similar to the occurrence of human OSCC at the genetic and molecular level. A review of molecular alterations at various stages of 4NQO-induced oral carcinogenesis had been accomplished by Kanojia and Vaidya, which covered apoptosis-related proteins, cell cycle-related proteins, proteins of cell-cell interactions, and cytoskeletal proteins (40). To identify the genetic alterations of 4NQO-induced C57BL/6J mice during the development of lingual SCC, Liu et al. (64) induced C57BL/6J mice with 4NQO (50 mg/L in drinking water) and then harvested lingual mucosa samples from different stages, namely normal tissue (0 week) and early-stage (12 week) and advanced-stage (28 week), respectively. Through microarray and methylated DNA immunoprecipitation sequencing, the result of bioinformatics analysis revealed significant alterations in 63 hub genes and promoter methylation, including Tbp, Smad1, Smad4, Pdpk1, Camk2, Atxn3, and Cdh2. Of the 63 human orthologous genes, 100% were reported to be associated with human cancer, and up to 55.5% were relevant to human oral cancer. Schoop et al. (65) revealed that the immunopathology of the murine oral tumor was similar to that of the described human oral tumor through immunohistochemistry labeled with cyclin D1 and E-cadherin.

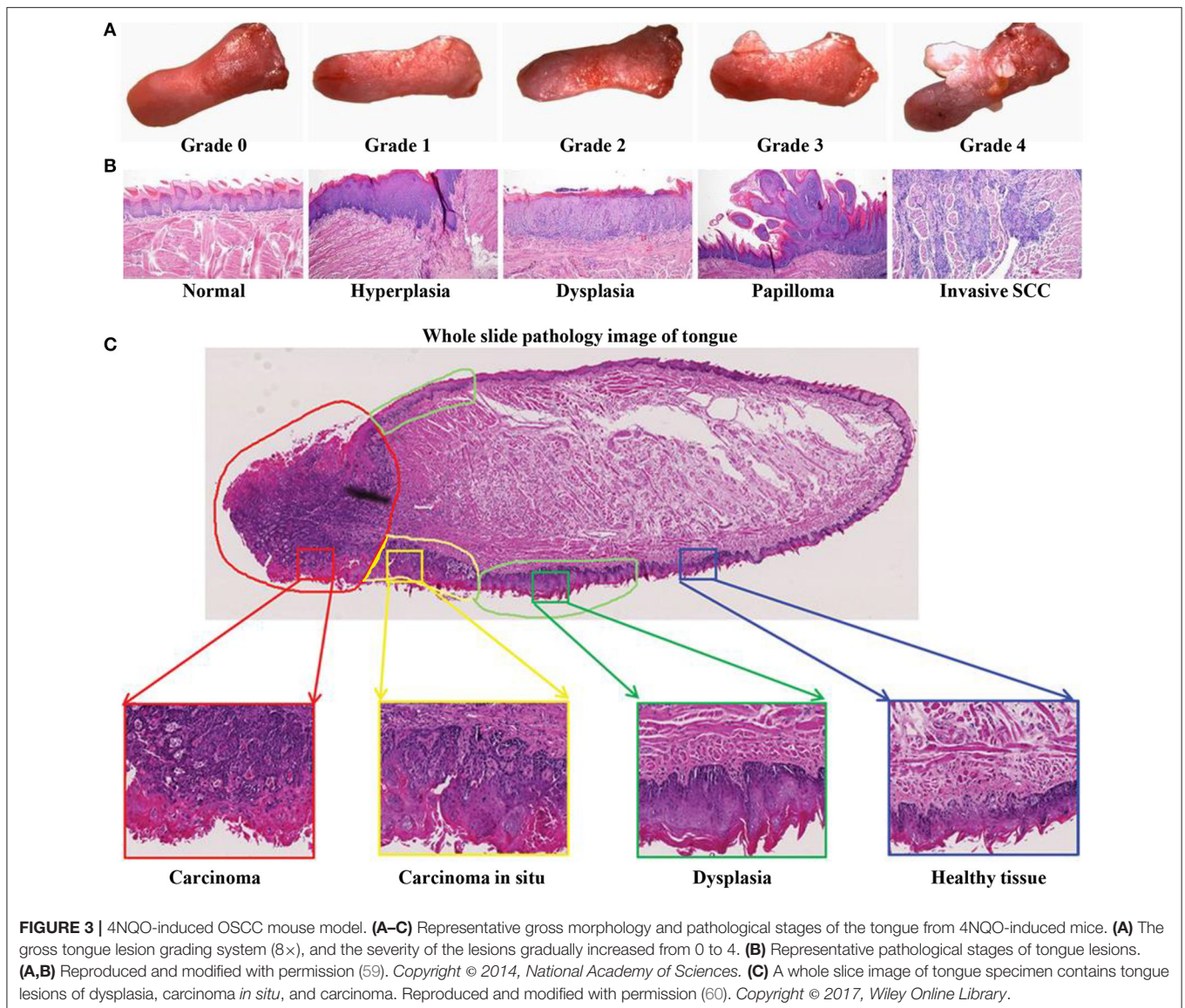
The carcinogenic effect of 4NQO starts with its reduction by 4NQO reductase, so the distribution and quantity of 4NQO

reductase in different tissues affect the tissue specificity of 4NQO carcinogenesis (66). 4NQO can induce carcinogenesis in many parts of the oral cavity, such as the dorsal tongue, ventral tongue, and palate (67, 68). Additionally, 4NQO passes from the oral cavity through the entire digestive tract, and the esophagus also contains a large amount of 4NQO reductase; therefore, this model can also form esophageal cancer (67, 69).

Methods for 4NQO-Induced OSCC Mouse Model

The strains of mice used for the 4NQO-induced OSCC mouse model include immunocompetent C57BL/6, BALB/c, CF-1, and CBA mice (Table 1). Most studies that have applied this method used adult mice aged 6–8 weeks, but Vincent-Chong et al. (76) observed that 92% of old mice (aged 65–70 weeks) developed severe dysplasia/invasive squamous cell carcinoma, while the incidence in young mice (aged 7–12 weeks) was 69%. CBA mice have been reported to be more susceptible to 4NQO induction than C57BL/6 mice (67, 77). Tang et al. (67) used 4NQO in drinking water to induce C57BL/6 and CBA mice and found that both strains developed a variety of precancerous lesions and carcinogenesis in the tongue and esophagus. CBA mice were treated with 50 and 100 $\mu\text{g}/\text{mL}$ 4NQO for 8 weeks, and 100% of them developed tongue lesions, and 100 $\mu\text{g}/\text{mL}$ 4NQO treatment for 8 or 16 weeks resulted in carcinogenesis of the tongue and esophagus. After 16 weeks of treatment with 100 $\mu\text{g}/\text{mL}$ 4NQO, tongue lesions were observed in 100% of C57BL/6 mice, but visible gross lesions were not seen until the following 4–12 weeks.

Administration of 4NQO can be carried out by topical application or the addition to drinking water, and both



methods have successfully established the OSCC mouse model (65, 76, 78–81). Initially, researchers used localized smearing of 4NQO to induce OSCC, which was the same approach used to induce SCC in hamster pouches by DMBA (65, 80). Schoop et al. (65) smeared the tongues of male CBA mice with 4NQO (5 mg/mL) dissolved in propylene glycol for 16 weeks, with three treatments every week. From 24 to 40 weeks, the researchers detected the continuous development of hyperplasia; mild, moderate, and severe dysplasia; and squamous cell carcinoma. The smear method ensures that 4NQO acts on the oral cavity to a great extent and reduces the 4NQO burden in the digestive tract as much as possible. However, some researchers have recently used drinking water containing 4NQO to establish the OSCC model since it is a more natural means of administration, faster to model, and less painful to the mice than the topical application method (76, 78, 79, 81).

As shown in **Table 1**, the dosage and administration time of 4NQO used by the drinking water method in different studies are diverse. The most commonly used 4NQO concentrations in drinking water to induce OSCC are 50 and 100 $\mu\text{g}/\text{mL}$ (61, 70). In general, a higher concentration means the establishment of OSCC is faster. Typically, the mice are exposed to 4NQO in the drinking water for about 16 weeks (treatment period) and then provided with normal drinking water for an additional 6–16 weeks (development period) (76, 78, 79, 81). There is no unified standard for the establishment of 4NQO-induced OSCC mouse models at present. Researchers can adjust these factors according to the purpose of the study. Tang et al. (67) administered different concentrations of 4NQO in drinking water to CBA mice: 100 $\mu\text{g}/\text{mL}$ 4NQO for 16 weeks, 100 $\mu\text{g}/\text{mL}$ for 8 weeks, 50 $\mu\text{g}/\text{mL}$ for 8 weeks, and 20 $\mu\text{g}/\text{mL}$ for 8 weeks. Of the four groups, 100% of the first three groups developed oral cavity lesions; the values of the bromodeoxyuridine (BrdUrd) labeling

TABLE 1 | Methods of 4NQO-induced mouse models in drinking water for OSCC.

The concentration of 4NQO ($\mu\text{g/mL}$)	Treatment period (/weeks)	Development period (/weeks)	Mouse strains	References
50	20	4	BALB/c	(70)
50	16	4 or 8	C57BL/6	(71)
100	16	4, 8, or 10	C57BL/6NCR	(13)
100	16	12	C57BL/6	(61)
100	16	12 or 13	CF-1	(72)
100	8	4, 8, 12, or 16	CBA	(73)
100	8	10	C57BL/6	(74)
100	16	6 or 12	C57BL/6	(75)

index, which can be used to reflect the degree of malignancy of oral cavity lesions, were $21.0 \pm 0.9\%$, $15.1 \pm 0.8\%$, $10.9 \pm 0.8\%$, and $11.1 \pm 0.5\%$, respectively, for the four groups.

Usage of 4NQO-Induced OSCC Mouse Model

Since the similarities of the 4NQO-induced OSCC mouse model in pathogenesis, pathological changes, and host immune activity, and molecular level to those of humans, this model is widely used to study OSCC, especially in developing the biomarkers for early diagnosis and the transformation of the epithelium. Because 4NQO simulates tobacco-related gene mutation and can induce primary OSCC, this model has been used to explore the pathogenesis of OSCC (82). A spontaneous tumor has a more natural tumor microenvironment (76, 83) and can also be used in the study of cytokines (61), mesenchymal stem cells (84), natural killer (NK) cells (85, 86), microbiomes (7), and angiogenesis (87). The murine lesions induced by 4NQO constitute a dynamic and continuous process and can be used to study the early detection and prevention of precancerous OSCC lesions (88–90). The immune activity of this model renders it suitable for researching the changes in tumor immunology in the process and development of tumorigenesis, as well as related subjects such as immunosuppression (91–94) and immunotherapy (34, 95, 96). In conclusion, the 4NQO-induced OSCC mouse model appears to be the best available model for research the diagnostic and prognostic markers for OSCC. However, this model has limited application for studies on the invasion and metastasis of malignant tumors because of its low probability of metastasis and bone invasion.

Other Chemical Carcinogen-Induced OSCC Mouse Models

Tobacco-Related Chemical Carcinogens-Induced OSCC

Benzo[a]pyrene (B[a]P)

B[a]P, a member of the PAHs family and a procarcinogen, is widely distributed in tobacco smoke, charcoal-grilled foods, contaminated water, engine exhaust, and soil (97). In a 2-year bioassay of female B6C3F1 mice, Culp et al. (35) compared the effect of coal tar and B[a]P on tumor induction and discovered that the mice fed with 100 ppm B[a]P developed tongue lesions (papillomas and carcinomas) with an incidence of 23/48. However, the main target of B[a]P is the forestomach.

Although high doses of B[a]P can induce tongue cancer, the toxicity of B[a]P is high, and the low carcinogenic specificity of B[a]P will produce lesions in other parts of the body, including the liver, lung, forestomach, esophagus, and larynx, which limit its application.

Dibenzo[a,l]pyrene (DB[a,l]P)

DB[a,l]P is a potent carcinogen produced in cigarette smoke and has been used to induce carcinogenesis of the lung, skin, mammary gland, and oral cavity in mice and rats (36, 98–100). Guttenplan et al. (36) revealed that a 24 nmol dose of DB[a,l]P by topical application to the oral cavity resulted in neoplasia in 31% of B6C3F1 mice, accompanied by the elevated expression of p53 and COX-2 protein. Furthermore, DB[a,l]P induced ovarian tumors.

DB[a,l]P and N'-nitrosornicotine (NNN)

Guttenplan et al. (37) compared the carcinogenesis and mutations resulting from the administration of DB[a,l]P, NNN, and both NNN and DB[a,l]P. DB[a,l]P (0.16 μmol) was topically applied on the tongue of *lacI* mice three times per week, while NNN (8.46 μmol) was applied two times per week. After induction for 5 weeks and development for 4 weeks, the mice were euthanized. This study revealed that DB[a,l]P + NNN caused the highest percentage of genetic mutations.

4NQO Combined With Other Chemical Carcinogens

4NQO and arecoline

Arecoline is an alkaloid extracted from betel nut and plays an essential role in the progression of oral cancer (101, 102). Chang et al. (38) treated C57BL/6JNarl mice with arecoline, 4NQO, or both arecoline and 4NQO for 8 weeks to induce oral carcinogenesis. They found that 100% of the mice induced by both 4NQO (200 $\mu\text{g/mL}$) and arecoline (500 $\mu\text{g/mL}$) developed tongue tumors, while 57 and 0% of the mice exposed to only 4NQO or arecoline developed tongue tumors, respectively. Similar to the results in human studies (103), immunohistochemical analysis revealed the expression of αB -crystallin and Hsp27 in this mouse tumor model. In this model, the mouse oral cavity was exposed to 4NQO and arecoline at the same time, simulating the etiology for oral cancer associated with betel nut.

4NQO and ethanol

Alcohol is another risk factor for oral cancer. Guo et al. (39) treated male wild-type C57BL/6J mice and 5-Lox knockout mice (*Alox5^{tm1Fuj}/J*) with 100 µg/mL 4NQO in drinking water for 8 weeks, and then in the following 16 weeks, 8% ethanol was provided *ad libitum* as the sole drink water. The incidence of OSCC increased from 20 (no ethanol) to 43% (8% ethanol) in wild-type mice, while fewer cancers were induced in the 5-Lox knockout mice. This study revealed that ethanol could promote 4NQO-induced oral carcinogenesis in mice by activating the 5-LOX pathway of arachidonic acid metabolism.

TRANSPLANTED OSCC MOUSE MODELS

Transplanted mouse models can be more accurately named “animal cultures” because tumor cells or tumor tissues are transferred to mice for culture. As early as 1969, Rygaard (104) successfully transplanted human malignant tumors into nude mice for the first time, which offered a new prospect in the research and application of transplanted mouse models.

Xenograft OSCC Mouse Models

Classifications of Xenograft OSCC Mouse Models

In tumor xenograft mice, tumor tissue or cell lines from one species are propagated in ectopic or orthotopic sites in immunodeficient mice (29). As shown in **Table 2**, depending on the source of the graft, xenograft mouse models can be divided into cell-derived xenografts (CDX) and patient-derived xenografts (PDX), which are derived from tumor cells cultured *in vitro* and fresh tumor tissues from patients, respectively. Xenograft mouse models can also be divided into ectopic or orthotopic mouse models depending on the tumor location. In ectopic mouse models, tumor cells are subcutaneously injected into the flank or back, while in orthotopic mice, tumor cells are typically transplanted to the tongue of mice.

Characteristics of Xenograft OSCC Mouse Models

A xenograft can be continuously transplanted in the same species or the same strain of animal, and the characteristics of easy replication, a high modeling success rate, and high stability facilitates the generation of abundant experimental mice.

The prominent characteristic of CDX models is high tumor consistency: after inoculating a certain number of tumor cells into mice, the volume and growth rate of the tumor are consistent, the inter-individual difference is low, and the effects on the hosts are identical (**Figures 4A–D**). But the transplanted tumor microenvironment lacks surrounding tissues, especially the stromal cells, vascular and lymphatic circulation, and immune cells of human origin (**Figure 4D**) (105, 106). Because different immunodeficient mice are used, the xenograft tissue lacks the structure of a typical immune system, although the immune cells are not absent. HE staining of HSC2-bearing tongues, dissected from athymic nude mice injected with HSC2 cells, revealed an immune reaction that included neutrophils, lymphocytes, and macrophages (107). CDX models can be considered PDX models with too many generations to be traceable. After multiple generations, the heterogeneity in the

genetic, histological, and phenotypic characteristics of the tumors causes gradual differences from the original tumor tissue (108). For this reason, the US National Cancer Institute (NCI) retired the NCI-60 panel—60 human tumor cell lines established by NCI—from the drug-screening program (109). PDX models can more accurately reflect the mechanism of tumor occurrence and development in patients. In contrast to the traditional CDX models, PDX models preserve the genotypic and phenotypic diversity of tumor tissue to reflect the characteristics of the original tumor genuinely. PDX models also maintain tumor stromal cells and tumor microenvironment (**Figures 4F–H**). In a previous study, HE and immunohistochemistry (IHC) staining revealed that the histopathology and IHC were highly consistent between the PDX models and the corresponding patients (112). However, after the secondary transfer of the PDX tumor, the tumor stroma disappeared rapidly and was replaced by mouse interstitial cells (113).

The ectopic OSCC model can be established by subcutaneous injection with little effort; the operation is simple, and the observation of ectopic tumors and the measurement of tumor volume are also intuitive. Furthermore, the growth of subcutaneous tumors is not limited by the oral cavity size of mice (**Figure 4C**). However, the anatomical structures of the oral cavity and the subcutaneous tissue have some differences, such as the vascular distribution, lymphatic reflux, and bone adjacency. The orthotopic model can provide an experimental environment more similar to the original tumor environment than the ectopic model (28). Besides, more aggressive behaviors of regional and distant metastasis were discovered in the orthotopic models (114, 115). However, the growth of intra-oral tumors in the orthotopic model will not only cause pain but also hinder the diet of mice, which is against humanitarianism. Fitch et al. (116) firstly established an orthotopic model of human OSCC cell lines. Tumor cells were extracted from tumors growing subcutaneously and then injected into the tongue of nude mice. Equal tumorigenicity of tumor cells was finally detected in oral and subcutaneous tissues. In contrast, Myers et al. (117) compared the tumorigenicity of three human OSCC cell lines, Tu159, Tu167, and MDA1986, in the orthotopic tongue and ectopic subcutaneous tissues. It was found that all three types of SCC were more likely to develop in orthotopic than ectopic. The local tumor growth, regional lymph node metastases, and distant visceral metastases of the established orthotopic nude mouse model showed similar histopathology and biological characteristics to the patient’s primary tumor.

Methods of Xenograft OSCC Mouse Models

The mice used in this model need to be immunodeficient because xenografts can otherwise trigger an immune response and cause a rejection reaction and graft-vs.-host disease (GvHD). The commonly used immunodeficient mice are athymic nude mice, severe combined immune deficiency (SCID) mice, non-obese diabetes–severe combined immune deficiency (NOD-SCID) mice, and NOD-*Prkdc^{scid}IL2rg^{null}* mice, such as NOD.Cg-*Prkdc^{scid}IL2rg^{tm1Sug}/Shi*J mouse (NOG) and NOD.Cg-*Prkdc^{scid}IL2rg^{tm1Wjl}/Sz*J mouse (NSG). Different gene mutations cause varying degrees of immunodeficiency in

TABLE 2 | Classifications of Xenograft mouse models.

Basis of classification	Classification	Advantages	Disadvantages
The source of the graft	CDX	Readily available cell lines, vast published literature for reference, and low cost	Tumor heterogeneity was significantly different from the original tumor tissue
	PDX	Tumor heterogeneity was stably retained	Complicated operation unrepeatable modeling, long construction time, high cost, and unstable success rate
The tumor location	Ectopic	Time-saving and less labor	Tumors formed in ectopic sites Rare metastasis and bone invasion are
	Orthotopic	Develop tumors in the oral region Develop bone invasive and distant metastasis	Harder implantation than ectopic xenograft More painful for mice

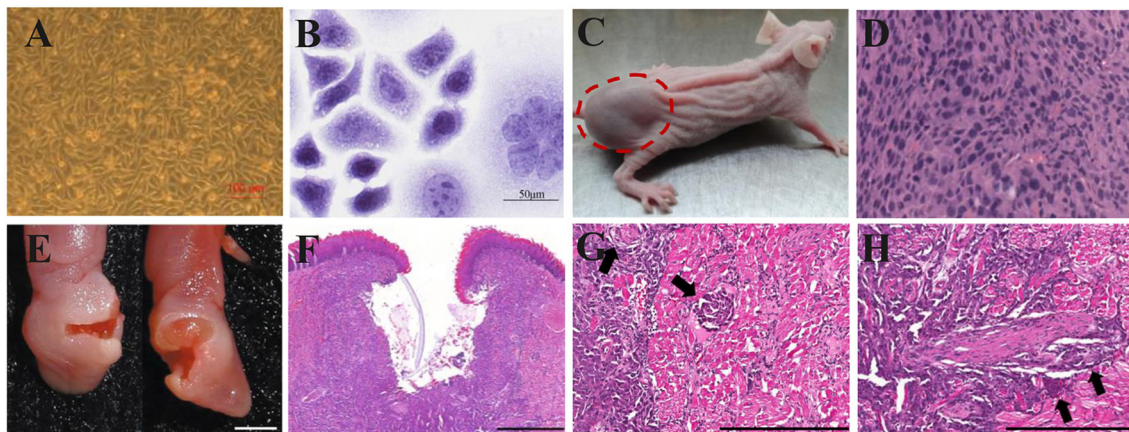


FIGURE 4 | Xenograft OSCC mouse models. **(A–D)** An ectopic mouse model of OSCC. **(A)** OSCC-BD cells overlapped and lost contact inhibition. **(B)** HE staining showed that OSCC-BD cells had malignant characters. **(C)** The nude mice were subcutaneously injected with OSCC-BD cells. Tumor formation was observed, and neoplasms were about 1.0 ± 0.2 cm in size. **(D)** HE staining showed the neoplasm was typical squamous cell carcinoma. Scale bars, $100 \mu\text{m}$ **(A)** and $50 \mu\text{m}$ **(B)**. Reproduced and modified with permission (110). Copyright © 2015, Springer Nature. **(E–H)** An orthotopic mouse model injected into the lateral border of the tongue of non-obese diabetes–severe combined immune deficiency (NOD-SCID) mice via HSC-3 cells. The HSC-3 bearing tumors have **(E,F)** ulcers. **(G)** neural, and **(H)** vascular invasion (arrows). Scale bars, 0.2 cm **(E)**, $400 \mu\text{m}$ **(F)**, and $200 \mu\text{m}$ **(G,H)**. Reproduced and modified with permission (111). Copyright © 2018, Springer Nature.

the four kinds of mice. Comparisons by various researchers have revealed that the mice with the highest potential for successfully engrafting and investigating human cancers are the immunodeficient *IL2rg^{null}* mice, followed by NOD-SCID mice, SCID mice, and athymic nude mice, in descending order of efficacy (Table 3) (118–120).

In ectopic mouse models, tumor cells are subcutaneously injected into the flank or back, while in orthotopic mice, tumor cells are mainly transplanted into the tongue of mice. Moreover, the orthotopic OSCC mouse model can also be established at the floor-of-mouth (FOM) region (126–128). Transplanting tumor cells into the FOM region allowed the tumor to occur in the submental region of the jaw rather than in the mouth, in order to create a tumor that was easier to surgically remove and avoided inevitable complications if a trans-oral resection was attempted (127).

CDX models are developed using established human-derived cell lines, such as the human oral carcinoma cell lines SCC9 (1×10^7 cells) (129), UM-SCC47 (1×10^6 cells) (130), CAL27-DsRed

(0.5×10^6 cells in $40 \mu\text{L}$ per tongue) (131), and UMSCC2-DsRed (0.5×10^6 cells in $40 \mu\text{L}$ per tongue) (131) (Table 4). The construction of PDX models has four phases (P): surgical removal of the tumor (P_0), engraftment (P_1), expansion (P_2), and treatment ($P_3 \dots P_n$). The tumor tissue obtained from surgery is cut into fragments (diameter of about 1 mm), mixed with Matrigel, and then transplanted into immunodeficient mice. When the tumor grows to a specific size, the tumor is removed and then re-transplanted for tissue expansion. The growth rate of each cell line or tumor tissue derived from different patients varies, and the time required for the successful construction of the transplanted tumor has differed among studies. Therefore, the endpoint of tumor growth is evaluated by the volume of the tumor (Table 4).

Usage of Xenograft OSCC Mouse Models

The development of xenograft mouse models has enabled the study of human tumor tissues and cell lines *in vivo* in immunodeficient mice. In light of the advantages as mentioned

TABLE 3 | Four kinds of immune-deficient mice (118–125).

Mouse species	Genetic backgrounds	Immunodeficiency	Life span	Main features
Athymic nude mouse	Homozygous nu/nu mutant mice; spontaneous deletion in the Foxn1 gene	Lack of functional T lymphocytes	18 months to 2 years	Hairless, naked, and athymic
SCID mouse	A spontaneous mutation in C.B-171c (C.B17) mice termed “SCID” (Prkdc ^{scid}), or express the Rag1 ^{null} or Rag2 ^{null} mutations	Lack of mature T and B lymphocytes	Above 1 year	“leaky,” can generate a certain degree of functional T and B cells with the increase of age
NOD-SCID mouse	Backcross the SCID mutation onto NOD mouse strain background	Lack of functional T and B lymphocytes. Lower NK cell activity, reduce levels of macrophage activation, abnormal DCs development and an absence of hemolytic complement	8 to 9 months	Less “leaky”; has spontaneous lymphoma
NOD-Prkdc ^{scid} IL2rg ^{null} mouse	NOD genetic background, Prkdc ^{scid} , and a targeted mutation in the IL2-receptor common gamma chain gene (IL2rg ^{null})	Lack T, B, and NK cells and have functionally impaired DCs and macrophages	1.5 years	No B lymphocyte leakage

TABLE 4 | Xenograft OSCC mouse models.

Classification	Cell lines / tissue source	End point	Mouse strains	Ref.
PDX	Patients with HNSCC	Xenografts reached 100 mm ³ to 200 mm ³	NSG mice	(130)
CDX	UM-SCC47 cells (1 × 10 ⁶ cells)	Xenografts reached 100 mm ³ to 200 mm ³	Nude-Foxn1 ^{null} mice	(130)
CDX;Orthotopic	CAL27-DsRed cells (0.5 × 10 ⁶ cells in 40 μl per tongue) UMSCC2-DsRed cells (0.5 × 10 ⁶ cells in 40 μl per tongue)	CAL27 tumors grew up to 25 ± 6 mm ³ by day 31 UMSCC2 tumors grew up to 20 ± 5 mm ³ by day 31	Nude mice (NCr ^{nu/nu})	(131)
PDX; Ectopic (bilaterally subcutaneous)	Three patients with HNSCC	A volume of 2,000 mm ³	SCID mice	(132)
PDX; Ectopic (in the flank)	HNSCC patients (25 mg of tumor/mouse)	A volume of 1 cm maximum diameter	NOD/SCID gamma mice	(133)
PDX; Ectopic (subcutaneous)	OSCC of right retromolar trigone, T ₃ N ₀ M ₀ and tongue—SCC, T ₁ N _{2b}	About 30 days	SCID mice	(134, 135)
PDX; Ectopic (subcutaneously on the flank)	Two patients with oral cancer T ₄ N ₀ M ₀ and T ₂ N ₂ M ₀	A volume of 1,000–1,500 mm ³	Nude mice	(136)

above of “animal cultures” of tumor cells or tissues *in vivo*, most antineoplastic drugs have been tested using xenograft mouse models in the preclinical stage. Compared with CDX models, PDX models are more advanced preclinical oncology models for new drug development and can achieve better preclinical drug efficacy testing and analysis. As the tumor model closest to the actual conditions of the human body, the PDX model can provide personalized drug guidance for a single patient and realize precision therapy for a tumor. In the field of OSCC research, xenograft OSCC mouse models are used for screening drugs (137–139) and studying drug resistance, such as cisplatin (9, 140), 5-fluorouracil (141), and cetuximab (142). Potential therapeutic targets of OSCC can also be verified in xenograft mouse models (143, 144). Researchers have also focused on invasion and metastasis (145–149), new techniques for detecting tumors (138), postoperative recurrence (127, 128), and comparisons with other models or primary tumors (132,

150). Nevertheless, xenograft mouse models are incapable of simulating the tumor microenvironment and cannot be used to study the interaction between tumors and host immunity because of the use of immunodeficient mice.

Syngeneic OSCC Mouse Models

Syngeneic OSCC mouse models are derived from the allografts of immortalized mouse tumor cell lines, chemical carcinogen-induced spontaneous mouse tumors, or genetically engineered mouse models (GEMMs). Syngeneic mice can effectively avoid tissue rejection and GVHD caused by the transplantation of tumor cells into allogeneic mice. The models also have the inherent advantages of transplanted tumor models, such as the high speed of establishment, high consistency, and high stability. These models can better reflect the tumor microenvironment and more comprehensively simulate the complexity of the tumor. Therefore, they are widely used in the study of oncoimmunology

and show great potential in the development of novel therapy for OSCC, especially immunotherapy.

Syngeneic Models Derived From Murine OSCC Cell Lines

The principle of syngeneic models derived from murine cell lines is similar to that of the CDX model. Various murine cell lines have been used to establish syngeneic OSCC mouse models, including murine squamous cell carcinoma SCC7 (151, 152), murine oral cancer (MOC) cell lines (153), and MOC1 (154), MOC2 (155), and murine OSCC Sq-1979 cells (156). Moroishi et al. (157) subcutaneously transplanted 1×10^5 SCC7 cells into both back flanks of C3H/HeOu mice and discovered that the tumor growth was aggressive, while all of the mice transplanted with LATS1/2 dKO SCC7 cells were tumor-free. Similarly, Dong et al. (152) subcutaneously injected 1×10^6 SCC7 cells into the right abdomen of C3H/HeJ mice to assess the therapeutic effect of the tumor-derived autophagosome vaccine (DRibble). To evaluate the antineoplastic effect of near-infrared photoimmunotherapy (NIR-PIT) produced by conjugating IR700DX (a photo-absorber) with anti-CD44 monoclonal antibodies, Nagaya et al. (153) built syngeneic models by subcutaneously injecting immunogenic MOC1 cells (2.0×10^6), moderately immunogenic MOC2-luc cells (1.5×10^5), and poorly immunogenic MOC2 mKate2 cells (1.5×10^5) into C57BL/6 mice. The authors ultimately demonstrated that NIR-PIT could significantly inhibit tumor growth in the three models. Similarly, Adachi et al. (156) subcutaneously injected 1×10^7 Sq-1979 cells into the posterior neck area of C3H/HeN mice to examine the genetic changes during the development of OSCC. In summary, these different murine OSCC cell lines were used to generate stable and straightforward syngeneic OSCC models successfully.

Syngeneic Models Derived From 4NQO-Induced Murine OSCC

Similar to the construction of the PDX model, Chen et al. (158) induced C57BL/6 mice with 4NQO (100 μ g/mL in drinking water) for 16 weeks, and the mice were sacrificed at the 28th week to establish the mouse tongue squamous cell carcinoma cell lines MTCQ1 and MTCQ2. After that, the cells were injected into the flanks and the tongues of C57BL/6 mice to establish ectopic and orthotopic mouse models, respectively. Compared with the human SAS tongue SCC cell line, the proliferation of MTCQ cells was lower, but the migration and invasion abilities were much higher than those of SAS cells. A subclone of GFP-labeled MTCQ1 cells was identified by immunostaining and fluorescence imaging, and extensive cervical lymph node metastasis and lung metastasis were discovered. Some treatment methods, such as miRNAs (particularly miR-134), cisplatin treatment, and anti-PD-L1 immunotherapy, also had therapeutic effects on this model. Besides, Chen et al. (159) used 4NQO-induced OSCC transgenic mice to establish a syngeneic model. K14-EGFP-miR-211 transgenic mice were induced by 4NQO (100 μ g/mL in drinking water) for 16 weeks and then sacrificed at set times. After that, the cell lines, designated MOC-L1 to MOC-L4, were established from the dissections of OSCC lesions on the dorsal

tongue surface. The cell lines were used to obtain orthotopic xenografts and perform real-time *in vivo* tumor imaging by injecting 5×10^6 cells into the central tongue portion of C57BL/6 mice. Additionally, the cells were used to analyze distant metastasis and assess the therapeutic efficacy of cisplatin.

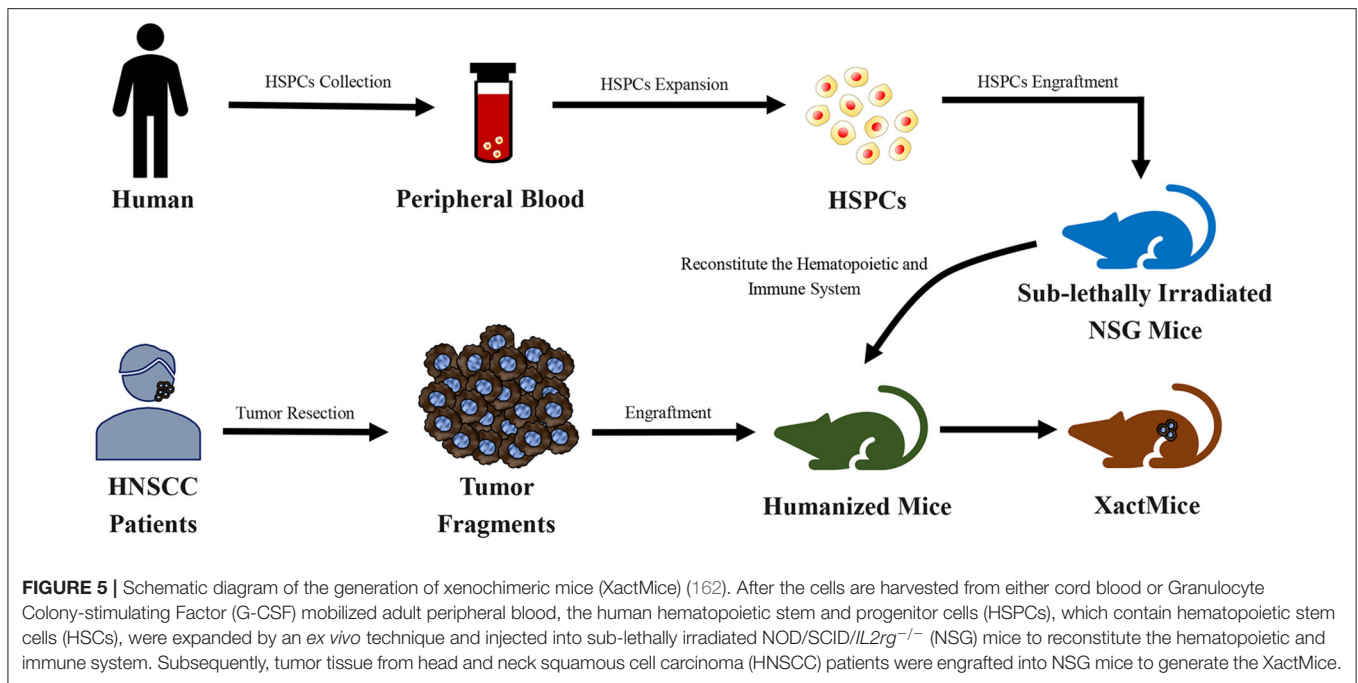
The immune system is a powerful weapon against a tumor, and the emergence and development of oncoimmunology have made conquering cancer an achievable goal. Syngeneic OSCC mouse models are feasible tools for oncoimmunology, but the major issue is that the models represent oral cancer in mice and form murine tumors with murine targets. There are significant differences in the composition and reaction mechanisms between mice and humans, and some targets in humans do not exist or respond in mice.

Humanized Mouse Models

The humanized mouse, which is developed by transplanting functional human cells or tissues into immunodeficient *Il2rg^{null}* mice, is an emerging preclinical model for studying human disease (160). For the study of tumors, current research focuses on [1] the establishment of novel tumor models (such as humanized CDX tumor models and humanized PDX tumor models) that are associated with human tumor-immune system interactions and [2] the exploration of therapy (including NK cell therapy, T cell editing, cytokine therapy, co-stimulatory enhancement, and checkpoint inhibitors) (161).

Morton et al. (162) reconstructed the tumor microenvironment in a humanized PDX mouse model of HNSCC (Figure 5). Tumors of a xenochimeric mouse (XactMice) presented human cells derived from humanized bone marrow, infiltration of human T and B cell populations, lymphangiogenesis, cytokine expression, and a dynamic microenvironment. Therefore, the XactMice system accurately recapitulates the growth of the original tumor *in vivo*. The humanized mouse model of HNSCC was optimized in another study by Morton et al. (163). After the dual infusion of human hematopoietic stem and progenitor cells (HSPCs) and mesenchymal stem cells (MSCs), the percentage of human immune cells in the bone marrow of established mice was almost twice that in mice implanted with HSPCs alone, and mature peripheral human immune cells were 9–38-fold more abundant. The dually engrafted mice also had more regulatory T cells, cytotoxic T cells, and MSCs. Thus, the dual infusion of HSPCs and MSCs resulted in a higher degree of humanization, which further increased the accuracy of the model.

As a new model, the technology of humanized mice is relatively immature, and the existing humanized immune mouse model system undeniably has many shortcomings. For instance, the immune response in the humanized mouse may be the result of tissue incompatibility (164). The transplanted human immune cells, mainly T cells, will produce GvHD and an immune attack on recipient mice and subsequently cause their death, so the operating window for conducting experiments is short (165). Nevertheless, the humanized mouse is entirely in line with the need to build a copy of the disease, so it remains a positive direction for the development of mouse models in the future.



Transplanted Mouse Models of HPV-Related Oral Cancer

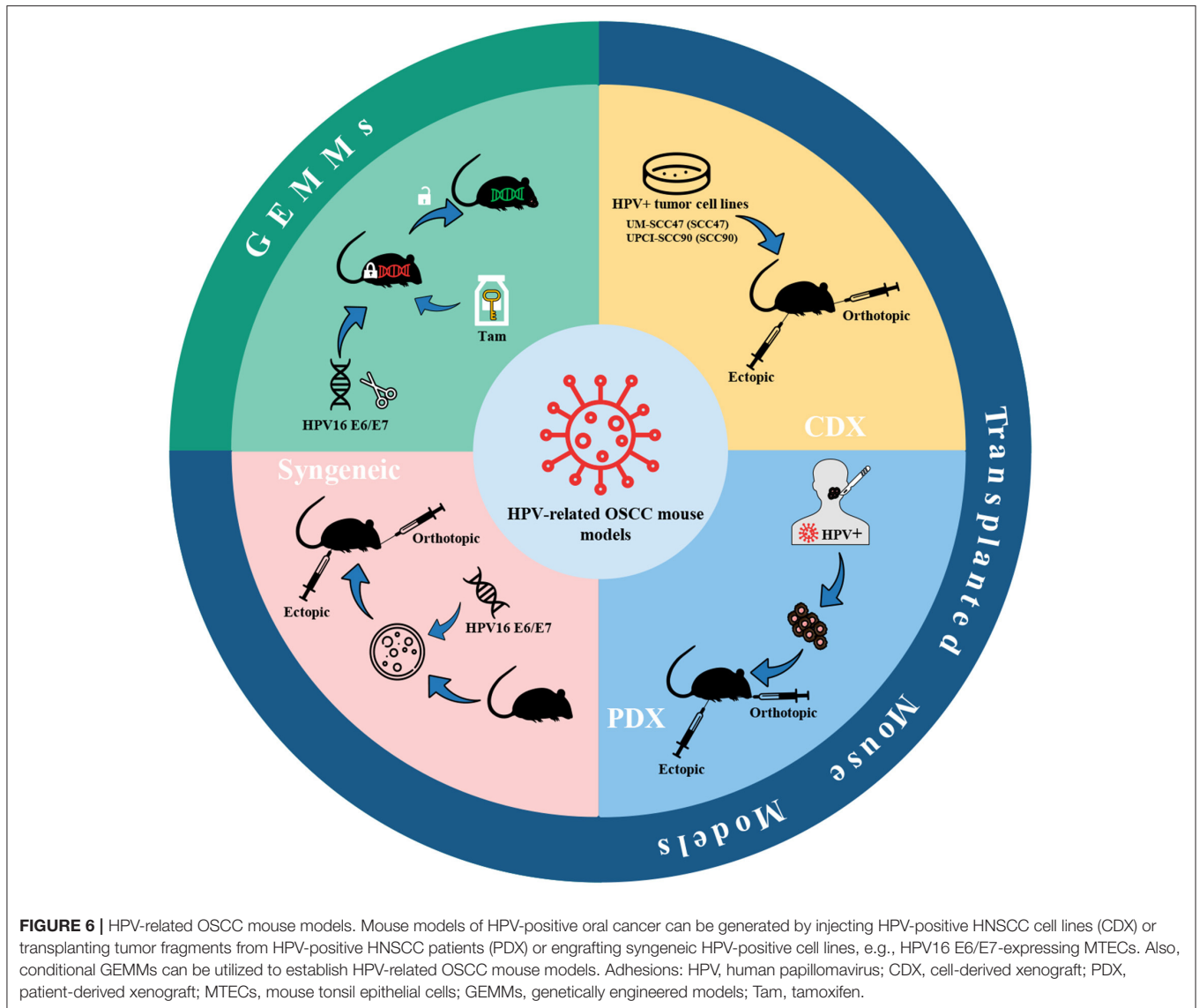
The HPV infection is one of the risk factors for HNSCC, and the incidence of HPV-related oropharyngeal squamous cell carcinoma (OPSCC) increases sharply in men under the age of 50 (166). Within 20 years, the percentage of HPV-positive OPSCC in the United States and some European countries has risen from <20% to more than 70% (166). Given the transfer of the incidence of HNSCC to the HPV-positive population, HPV-positive oral cancer has aroused the interest of researchers, and the corresponding mouse models have been gradually developed. Currently, mouse models of HPV-positive oral cancer can be classified as transplanted models and genetically engineered mouse models (GEMMs) (Figure 6), the latter of which will be introduced in section GEMMs of HPV-related oral cancer.

The high-risk subtypes of HPV are mainly HPV16 and HPV18, while the former is considered to be associated with 90% of HPV-related cancers (167). The two proteins E6 and E7 in the early coding region of the HPV genome are highly conserved in high-risk HPV subtypes and are the most critical viral-encoded proteins involved in cancer (168). Thus, the current mouse models of HPV-related oral cancer mainly focus on the construction of cell lines or mouse strains expressing HPV16 E6/E7.

Brand et al. (169) established an HPV-related CDX model by bilaterally injecting HPV-positive HNSCC cell lines UM-SCC47 (SCC47) and UPCI-SCC90 (SCC90) into the athymic nude mice. The tumor fragments of HNSCC patients were also utilized to implant into NSG mice bilaterally to establish the PDX model. Keysar et al. (170) developed a model covering a total of 25 strains of HNSCC clinical spectrum, in which primary and recurrent tumors (including HPV-positive and HPV-negative)

from HNSCC patients were implanted on mice using a modified floor-of-the-mouth (FOM) or base-of-tongue (BOT) implantation protocol to produce orthotopic tumors. Through the continuous passage of these models, the tumors maintained their original morphology, genetic characteristics, and drug susceptibilities. The gene characteristics of these tumors were following the known mutation frequencies of TP53, PI3KCA, NOTCH1, and NOTCH2. In addition, Facompre et al. (171) have also verified an elevated level of expression of p16^{INK4A} and E6/E7 virus oncogene transcripts. Meanwhile, the barriers of HPV-related HNSCC PDX models were also summarized in the research of Facompre et al. including a low engrafted rate and the formation of Epstein-Barr virus-positive (EBV+) human large B-cell lymphomas. The biological characteristics of HPV-positive HNSCC are low degree of malignancy, low invasiveness, and weak growth potential of tumor cells *in vitro*, which lead to the paucity of available HPV-positive HNSCC cell lines (172). Accordingly, selection biases against the more typical molecular characteristics of HPV-positive tumors may occur during the experiments. Likewise, using less invasive tumors as xenografts may have adverse growth characteristics and further prevent PDX from remaining stable during continuous passage *in vivo* (171).

Another HPV-related mouse oral cancer model is generated by syngeneic HPV-positive cell lines. John Lee et al. (173) transferred retroviruses expressing HPV16 E6, E7, H-Ras, and an empty control vector into mouse tonsil epithelial cells (MTECs) to construct stable murine HPV-related cell lines *in vitro*. After that, 5×10^5 cells were injected into the tongue of C57BL/6 mice, or 1×10^6 cells were injected into the subcutaneous tissue of the upper back near the spine. It turned out that only HPV16 E6/H-Ras MTECs and HPV16 E6/E7/H-Ras MTECs formed invasive tumors in syngeneic C57BL/6 mice at orthotopic



and ectopic sites. On this basis, in order to investigate whether HPV-specific immune mechanisms can result in tumor clearance, Williams et al. (174) developed preclinical models by injecting 1×10^6 HPV16 E6/E7/H-ras MTECs or HPV-negative cells subcutaneously on the right flank of C57BL/6 or SCID mice. Moreover, Mermod et al. (175) developed a novel HPV-positive HNSCC mouse model in which 1×10^5 HPV16 E6/E7-expressing MTECs were transplanted into the submental region of the FOM. After that, the tumor was surgically removed to investigate the progress of postoperative primary tumor recurrence and regional lymph node metastasis. Similarly, Paolini et al. (176) established HPV16 E7 expressing mouse OSCC AT-84 cells (AT-84 E7 cells) and AT-84-E7 luminescent cells. Then 6×10^5 AT-84 cells were injected into the FOM to obtain orthotopic tumors. Despite widely used, a major concern in syngeneic mouse models is the representativeness of mouse-derived tumor cells to human-derived tumor cells.

Although transplanted mouse models are currently the most commonly used animal models of HPV-related oral cancer, and their successful establishment has been documented in several publications, the lack of an appropriate HPV-positive mouse model—remaining stable during continuous passage *in vivo* and possessing more molecular characteristics with HPV-positive tumor cells of human origin—is still an obstacle to preclinical evaluation and treatment.

GENETICALLY MODIFIED MOUSE MODELS

Genetically modified mouse models, also known as genetically engineered mouse models (GEMMs), are intricate and novel animal models that have been a beneficial outcome of the development of genetic engineering technology. A review of

GEMMs of OSCC was published by Ishida et al. (177), so we mainly provide an overview of GEMMs.

An Overview of GEMMs

Classifications of GEMMs

GEMMs can be classified as either loss of function or gain of function. Loss of function entails gene knockout or knockdown, in which the expression of target genes is depleted or silenced. In the field of oncology, the blocked genes are typically oncogenes, tumor-suppressor genes, and metabolic genes (178). Gain-of-function studies use knock-in models of oncogene overexpression to study the function of an oncogene *in vivo*. According to the specificity, GEMMs can be classified as either conventional GEMMs or conditional GEMMs. Conventional GEMMs alter the gene of interest in every cell in the body, which is inconsistent with the reality where multiple mutational gene sites in a single cell suppress cell apoptosis and promote proliferation, resulting in tumorigenesis (179). Because of the spatiotemporal specificity of conditional GEMMs, their genes can be altered in different tissues or periods using conditional genetically modified techniques.

Characteristics of GEMMs

GEMMs enable the editing of specific genes through the activation or overexpression of oncogenes and the inactivation or silencing of tumor-suppressor genes. The pathological changes in these GEMMs, including hyperkeratosis, abnormal hyperplasia, carcinoma *in situ*, and invasive carcinoma (180–184), are similar to those of primary OSCC in humans and 4NQO-induced OSCC in mice. By the age of 5–6 months, histologic examination of L2D1⁺/p53^{+/-} and L2D1⁺/p53^{-/-} mice revealed hyperkeratosis, hyperplasia, severe epithelial dysplasia, and even cancer (181). Importantly, tumors of GEMMs grow in an environment with full immunity, so GEMMs are especially suitable for oncoimmunology study.

However, as a novel and promising model, there are still several barriers to the full application of GEMMs. Firstly, although the introduction of mice expressing Cre recombinase is driven by oral mucosa-specific promoters such as K5 or K14, the tumors generated by GEMMs have low specificity and appear in sites other than the oral cavity, such as the skin, tongue, esophagus, and forestomach (180, 181, 185, 186). Secondly, because of the full range of genetic changes caused by gene editing, GEMMs have a short lifespan and a high mortality rate, and highly malignant OSCC may not develop. For example, at 5 months, p53^{-/-} and L2D1⁺/p53^{-/-} mice had to be euthanized as a result of the morbidity caused by systemic lymphomas or sarcomas (181). Thirdly, the development of the human tumor is caused by mutations in a small number of cells surrounded by normal cells, while the introduction of exogenous genes or the knockout of endogenous genes in GEMMs will occur in all (conventional GEMMs) or most (conditional GEMMs) of the cells. Human tumors are usually accompanied by multiple mutations and metastases, which is not the case with GEMMs (187). Finally, the role of altered genes is questionable in the occurrence and development of OSCC. *Kras*, one of the most frequently used mutant genes in GEMMs of OSCC, has a low

mutation frequency in human HNSCC, while the *ras* family is accounting for only 5% (188, 189). Almost all HPV-positive oral cancer patients are p53 wild type (190), which indicates that GEMMs of OSCC generated by p53 gene mutation are not representative of HPV-positive oral cancer.

Methods of GEMMs

C57BL/6 is the first mouse strain to have its complete genome sequenced and is regarded as a “standard” inbred line, which can provide a genetic background for many mutant genes. Therefore, C57BL/6 is widely used as a transgenic mouse model to mimic human genetic defects in genetic experiments. Additionally, Balb/c mice can also be used as the genetic background of GEMMs (154).

The specificity of conditional GEMMs is controlled by the appearance of a recombinase, for example, the Cre-loxP recombinase system (Figure 7) (191, 192). The temporal specificity of conditional GEMMs is achieved through inducible promoters, which are regulated by exogenous chemicals, such as tamoxifen (180) and RU486 (185, 193). When the chemicals are present or removed, the promoters are activated, and then the expression of downstream target genes is changed (194, 195). The spatial specificity or tissue specificity in conditional GEMMs is determined by Cre transgenes that are expressed from tissue-specific promoters (29). For the oral cavity, the known optimal promoters are the keratin 5 (K5) and keratin 14 (K14) promoters (177). K5 is expressed within the basal layer of the tongue and forestomach stratified squamous epithelia, while K14 has been found to be expressed in the basal layer of the oral mucosa and tongue (185). Furthermore, a promoter of the Epstein–Barr virus, ED-L2, has been shown to target genes in oral and esophageal squamous epithelial cells (181, 196).

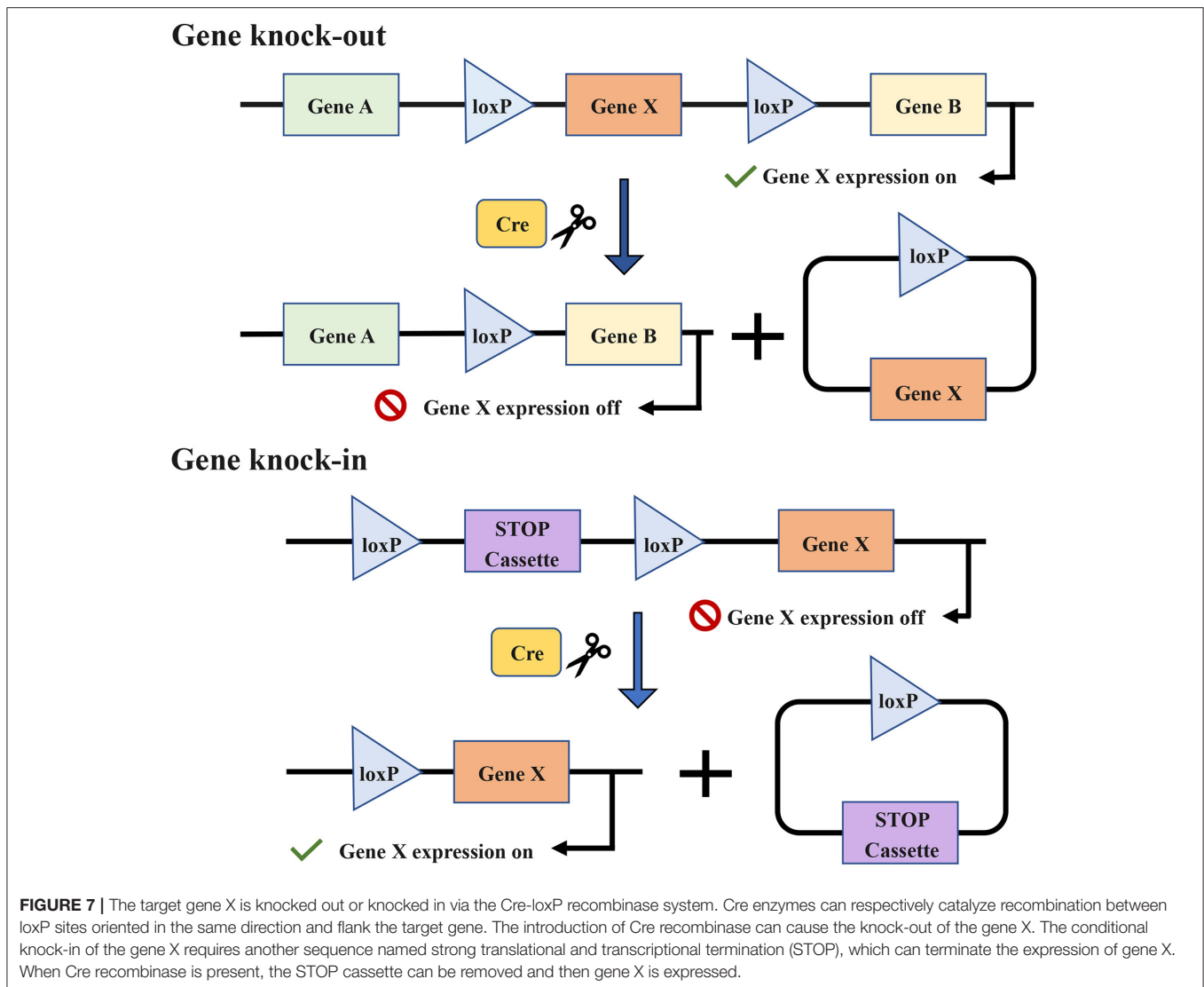
As shown in Table 5, the current GEMMs of OSCC are mainly conditional, the implementation of which mostly depends on the hybridization of the Cre mouse and gene-floxed mouse. Different genetic changes cause different cancer rates, and the carcinogenic time ranges from 10 weeks to 16 months. Generally, the activation of oncogenes or inhibition of tumor-suppressor genes accelerates the progression of carcinogenesis, while the activation of tumor-suppressor genes or the knockout of oncogenes will slow down or even halt carcinogenesis.

Usage of GEMMs

At present, several studies have induced oral carcinogenesis by changing the expression of oncogenes or tumor-suppressor genes and identified the links between genes and cancer. The simple GEMMs can be used to reveal novel mechanisms of carcinogenesis and will be an essential tool in the study of oral cancer-related gene mutations or proteins in the future. However, the high mortality caused by unexpected primary tumors limits its application in highly malignant OSCC.

4NQO-Induced Combined With GEMMs

Given that mice induced by 4NQO can develop spontaneous OSCC and precancerous lesions, some studies have combined 4NQO induction with GEMMs. This combined model integrates the advantages of both methods. Wild-type mice were used as



a control in the study of this combined model. The wild-type and genetically modified mice were induced by 4NQO (50, 100, or 150 $\mu\text{g}/\text{mL}$ in drinking water) for 8–30 weeks (Table 6). The effect of 4NQO on both mice reflected the effect of gene changes on OSCC, such as susceptibility and resistance.

In the combined model, in contrast to simple 4NQO induction, specific gene deletion or overexpression can be studied; compared with simple GEMMs, more specific OSCC can be induced, and genetic changes that are not directly carcinogenic can be investigated. This model can be used to study the role of miRNA (199, 200), proteins (82, 184, 203), and pathways (201, 202) involved in the carcinogenesis of OSCC. Furthermore, the knock-in of green fluorescent protein can be used to label cells with specific gene changes (158, 199).

GEMMs of HPV-Related Oral Cancer

By utilizing the tamoxifen-regulated Cre recombinase system, Zhong et al. (197) targeted HPV-16 oncogenes E6 and E7

and a luciferase reporter gene (iHPV-Luc) in epithelial cells of transgenic mice and established a preclinical model of autologous HPV-positive oral tumors (Table 5). Tamoxifen treatment in this model generated the development of oral tumors that detected the expression of HPV biomarkers p16 and MCM7, PIK3CA, and PTEN mutations following HNSCC sequencing data and an active mTOR-PI3K pathway. However, this GEMM still has some limitations in accurately reflecting the clinical conditions of HNSCC patients (197). First, Mutant *Kras* was required for the development of HPV-positive tumors, while the *ras* family mutations account for only about 5% of HNSCC cases. Second, the expression of HPV oncogene was artificially driven by a cytomegalovirus promoter and did not reflect human HPV positive tumors. Finally, HPV-positive mice developed oral tumors rather than oropharyngeal cancers commonly seen in HNSCC patients. Caper et al. (198) established a novel inducible GEMM of HPV-related OPSCC, in which the HPV16 oncogenes were activated in a tissue-specific and temporal

TABLE 5 | GEMMs for OSCC.

Mouse strains	Brief methods	Tumor formation/ conclusions	References
L2D1 ⁺ / <i>p53</i> ^{+/-} and L2D1 ⁺ / <i>p53</i> ^{-/-} mice	The Epstein-Barr virus ED-L2 promoter (L2) was used to generate the L2-cyclin D1 (L2D1 ⁺) mouse, which was crossed L2D1 ⁺ mice with <i>p53</i> ^{+/-} and <i>p53</i> ^{-/-} mice	Both models developed invasive oral-esophageal SCC by 6 months	(181)
LSL- <i>Kras</i> ^{G12D} ; K5 or K14-CrePR1	The <i>Kras</i> ^{G12D} oncogene driven by the K5 or K14 promoter was distributed under the control of Cre recombinase fused to a mutant of the human progesterone receptor	Administration of RU486 for 16–24 weeks induced the overexpression of oncogenic <i>K-ras</i> ^{G12D} in the oral epithelium of mice and resulted in the development of squamous papillomas in the oral cavity.	(185)
<i>Tgfb1/Pten</i> 2cKO mice	The <i>Tgfb1</i> ^{lox/lox} mice and <i>Pten</i> ^{lox/lox} mice crossed with mice driven by <i>K14-CreER</i> ^{tam}	After tamoxifen (tam) induction for 10 weeks, the <i>Tgfb1/Pten</i> 2cKO mice developed cancer and precancerous lesions in the oral epithelium.	(180)
<i>p53</i> ^{R172H} ; K5-CrePR1 and <i>p53</i> ^{lox/lox} ; K5-CrePR1 mice	The Neo- <i>p53</i> ^{R172H} and <i>p53</i> ^{lox/lox} mice crossed with K5-CrePR1 transgenic mice	By 15–16 months, <i>p53</i> ^{R172H} ; K5-CrePR1 (16%) and <i>p53</i> ^{lox/lox} ; K5-CrePR1 (25%) mice developed OSCC	(182)
LSL- <i>Kras</i> ; iHPV-Luc; K14-CreER ^{tam} mice (KHR mice) and LSL- <i>Kras</i> ; K14-CreER ^{tam} mice (KR mice)	The iHPV-Luc transgenic mice were established by knocking-in HPV16 E6E7 and a luciferase reporter on an FVB background. K14-CreER ^{tam} mice were backcrossed to the FVB background and then bred with iHPV-Luc mice to generate K14-CreER ^{tam} × iHPV-Luc (KH) mice. After that, KH mice were bred with LSL- <i>Kras</i> mice to produce KHR or KR mice.	Tamoxifen induced oral tumors in KR and KHR mice and the bioluminescence signal of KHR mice maximized 74.8 times higher than that of untreated mice.	(197)
HPV16 E7iresE6; <i>PIK3CA</i> ^{E545K} ; KRT14-CreER ^{tam} mice	Combined Rosa26-LSL-E7iresE6 and mutant <i>PIK3CA</i> (<i>Rosa26-LSL-PIK3CA</i> ^{E545K}) under the control of KRT14-CreER ^{tam} using intra-lingual tamoxifen delivery method	After the administration of tamoxifen for 6–8 weeks, oropharyngeal tumors developed with about 40% penetrance (1–2 tumors/tongue)	(198)

TABLE 6 | 4NQO induced combined with GEMMs for OSCC.

4NQO application and treatment period (weeks)	Mouse strains	Conclusions	Ref.
50 μg/mL 4NQO in drinking water for 16 or 30 weeks	<i>Ndr2</i> -deficient mice (<i>Ndr2</i> ^{+/-} and <i>Ndr2</i> ^{-/-} mice)	Tumors in <i>Ndr2</i> -deficient mice were significantly developed faster and larger.	(82)
100 μg/mL 4NQO in drinking water for 8 weeks	Heterozygous <i>p53</i> knockout mice (<i>p53</i> ^{+/-})	Anti-PD-1 can prevent OSCC development and progression.	(89)
150 μg/mL 4NQO in drinking water for 18 weeks	<i>Nlrp3</i> ^{-/-} and <i>Caspase1</i> ^{-/-} mice	NLRP3 inflammasome promoted 5-FU resistance of OSCC <i>in vivo</i> .	(141)
100 μg/mL 4NQO in drinking water for 16 weeks	K14-EGFP-miR-211 transgenic mice tagged with GFP	MicroRNA-211 enhances the oncogenicity of carcinogen-induced oral carcinoma by repressing TCF12 and increasing antioxidant activity.	(199)
100 μg/mL 4NQO in drinking water for 16 weeks	K14-EGFP-miR-31 transgenic mice tagged with GFP	The transgenic mice had a higher susceptibility for 4NQO-induced oral and esophagus tumorigenesis.	(200)
50 or 200 μg/mL in drinking water for 28 weeks	<i>CCL3</i> ^{-/-} mice; <i>CCR5</i> ^{-/-} mice; <i>CCR1</i> ^{-/-} mice	SCC tumor formation is reduced in <i>CCL3</i> and <i>CCR5</i> deficient mice.	(201)
100 μg/mL 4NQO in drinking water for 16 weeks	<i>Gal3</i> ^{-/-} male mice	In <i>Gal3</i> ^{+/+} mice, the Hh signaling pathway might play an essential role in tongue carcinoma development.	(202)
50 or 200 μg/mL 4NQO in drinking water for 28 weeks	<i>ACKR2</i> ^{-/-} mice	No differences in the SCC incidence comparing wide-type and <i>ACKR2</i> ^{-/-} treated mice.	(203)

manner *in vivo* (Table 5). The expression of HPV16 E6/E7 and the tissue-specific expression of mutant *PIK3CA*^{E545K} were induced by intra-lingual tamoxifen delivery, which replicated the histological and molecular characteristics of human HPV-positive OPSCC, including robust immune cell infiltration. Meanwhile, oropharyngeal lesions were accompanied by robust S6 phosphorylation at Ser235/236 in oropharyngeal tumors and low-level ERK1/2 activation (Thr202/Tyr204 phosphorylation).

CONCLUSIONS

In conclusion, mouse tumor-bearing models provide a preclinical study platform and make a significant contribution to the development of a cure for OSCC. A comprehensive understanding of model establishment is crucial for thoroughly studying OSCC. While it is impossible to replicate the actual situation of OSCC absolutely, mouse models can come very

close. Thus, each model should be considered on the premise of its shortcomings, and the appropriate model should be chosen according to their overall advantages. Furthermore, choosing the appropriate model based on the specific research purpose can improve research efficiency. In a single research study, several types of models can be mixed according to the research purpose to ensure the scientific robustness and correctness of the results.

AUTHOR CONTRIBUTIONS

QL, HD, YM, and YN: conceptualization. QL, HD, and GY: literature search. QL and HD: writing. HD: figure rendering. QL: table editing. QL, HD, GY, YS, YM, and YN: manuscript correction. All authors read and approved the final manuscript.

REFERENCES

- Park J, Zhang X, Lee SK, Song NY, Son SH, Kim KR, et al. CCL28-induced RAR β expression inhibits oral squamous cell carcinoma bone invasion. *J Clin Invest.* (2019) 129:5381–99. doi: 10.1172/JCI125336
- Fan H, Tian H, Cheng X, Chen Y, Liang S, Zhang Z, et al. Aberrant Kank1 expression regulates YAP to promote apoptosis and inhibit proliferation in OSCC. *J Cell Physiol.* (2020) 235:1850–65. doi: 10.1002/jcp.29102
- Jemal A, Bray F, Center MM, Ferlay J, Ward E, Forman D. Global cancer statistics. *CA Cancer J Clin.* (2011) 61:69–90. doi: 10.3322/caac.20107
- Sahu N, Grandis JR. New advances in molecular approaches to head and neck squamous cell carcinoma. *Anticancer Drugs.* (2011) 22:656–64. doi: 10.1097/CAD.0b013e32834249ba
- Sano D, Myers JN. Metastasis of squamous cell carcinoma of the oral tongue. *Cancer Metastasis Rev.* (2007) 26:645–62. doi: 10.1007/s10555-007-9082-y
- Gao P, Liu S, Yoshida R, Shi CY, Yoshimachi S, Sakata N, et al. Ral GTPase activation by downregulation of RalGAP enhances oral squamous cell carcinoma progression. *J Dent Res.* (2019) 98:1011–9. doi: 10.1177/0022034519860828
- Stashenko P, Yost S, Choi Y, Danciu T, Chen T, Yoganathan S, et al. The oral mouse microbiome promotes tumorigenesis in oral squamous cell carcinoma. *mSystems.* (2019) 4:e00323–19. doi: 10.1128/mSystems.00323-19
- Yang Z, Liang X, Fu Y, Liu Y, Zheng L, Liu F, et al. Identification of AUNIP as a candidate diagnostic and prognostic biomarker for oral squamous cell carcinoma. *EBioMed.* (2019) 47:44–57. doi: 10.1016/j.ebiom.2019.08.013
- Khoo XH, Paterson IC, Goh BH, Lee WL. Cisplatin-resistance in oral squamous cell carcinoma: regulation by tumor cell-derived extracellular vesicles. *Cancers.* (2019) 11:1166. doi: 10.3390/cancers11081166
- Kim SY, Han YK, Song JM, Lee CH, Kang K, Yi JM, et al. Aberrantly hypermethylated tumor suppressor genes were identified in oral squamous cell carcinoma. (OSCC). *Clin Epigenet.* (2019) 11:116. doi: 10.1186/s13148-019-0715-0
- Yoon M, Campbell JL, Andersen ME, Clewell HJ. Quantitative *in vitro* to *in vivo* extrapolation of cell-based toxicity assay results. *Critical Rev Toxicol.* (2012) 42:633–52. doi: 10.3109/10408444.2012.692115
- Warner BM, Casto BC, Knobloch TJ, Accurso BT, Weghorst CM. Chemoprevention of oral cancer by topical application of black raspberries on high at-risk mucosa. *Oral Surg Oral Med Oral Pathol Oral Radiol.* (2014) 118:674–83. doi: 10.1016/j.oooo.2014.09.005
- Vincent-Chong VK, DeJong H, Attwood K, Hershberger PA, Seshadri M. Preclinical prevention trial of calcitriol: impact of stage of intervention and duration of treatment on oral carcinogenesis. *Neoplasia.* (2019) 21:376–88. doi: 10.1016/j.neo.2019.02.002

FUNDING

This review was funded by the National Natural Sciences Foundation of China (Nos. 81772880 to YN, 81371680 and 81571800 to YM), Development of Science and Technology of Nanjing (No. 201803036 to YM), Jiangsu Provincial Medical Talent (No. ZDRCC2016016 to YM), Nanjing Medical Science and Technique Development Foundation (QRX17083, ZKX18035), and Nanjing Municipal Key Medical Laboratory Constructional Project Funding.

ACKNOWLEDGMENTS

The authors would like to thank the original authors of **Figures 3, 4** and all references for their significant researches contributing to this manuscript. Besides, the authors wish to thank MDPI English editing for their editing service.

- Khiavi MM, Abdal K, Abbasi MM, Hamishehkar H, Aghbali AA, Salehi R, et al. Comparison of injectable doxorubicin & its nanodrug complex chemotherapy for the treatment of 4-nitroquinoline-1-oxide induced oral squamous cell carcinoma in rats. *Indian J Med Res.* (2017) 145:112–7. doi: 10.4103/ijmr.IJMR_542_14
- Fulton AJ, Nemeč A, Murphy BG, Kass PH, Verstraete FJ. Risk factors associated with survival in dogs with nontonsillar oral squamous cell carcinoma 31 cases. (1990–2010). *J Am Vet Med Assoc.* (2013) 243:696–702. doi: 10.2460/javma.243.5.696
- Soltero-Rivera MM, Krick EL, Reiter AM, Brown DC, Lewis JR. Prevalence of regional and distant metastasis in cats with advanced oral squamous cell carcinoma: 49 cases. (2005–2011). *J Feline Med Surg.* (2014) 16:164–9. doi: 10.1177/1098612X13502975
- Rossa C, D'Silva NJ. Non-murine models to investigate tumor-immune interactions in head and neck cancer. *Oncogene.* (2019) 38:4902–14. doi: 10.1038/s41388-019-0776-8
- Manimaran A, Manoharan S. Tumor preventive efficacy of emodin in 7,12-dimethylbenz[a]Anthracene-induced oral carcinogenesis: a histopathological and biochemical approach. *Pathol Oncol Res.* (2018) 24:19–29. doi: 10.1007/s12253-017-0205-7
- Chen YK, Hsue SS, Lin LM. Correlation between inducible nitric oxide synthase and p53 expression for DMBA-induced hamster buccal-pouch carcinomas. *Oral Dis.* (2003) 9:227–34. doi: 10.1034/j.1601-0825.2003.02878.x
- Li N, Sood S, Wang S, Fang M, Wang P, Sun Z, et al. Overexpression of 5-lipoxygenase and cyclooxygenase 2 in hamster and human oral cancer and chemopreventive effects of zileuton and celecoxib. *Clin Cancer Res.* (2005) 11:2089–96. doi: 10.1158/1078-0432.CCR-04-1684
- Vidya Priyadarsini R, Kumar N, Khan I, Thiagarajan P, Kondaiah P, Nagini S. Gene expression signature of DMBA-induced hamster buccal pouch carcinomas: modulation by chlorophyllin and ellagic acid. *PLoS ONE.* (2012) 7:e34628. doi: 10.1371/journal.pone.0034628
- Shklar G. Development of experimental oral carcinogenesis and its impact on current oral cancer research. *J Dent Res.* (1999) 78:1768–72. doi: 10.1177/00220345990780120101
- Mognetti B, Di Carlo F, Berta GN. Animal models in oral cancer research. *Oral Oncol.* (2006) 42:448–60. doi: 10.1016/j.oraloncology.2005.07.014
- Salley JJ. Experimental carcinogenesis in the cheek pouch of the Syrian hamster. *J Dent Res.* (1954) 33:253–62. doi: 10.1177/00220345540330021201
- Smith LP, Thomas GR. Animal models for the study of squamous cell carcinoma of the upper aerodigestive tract: a historical perspective with review of their utility and limitations. Part A. Chemically-induced de novo cancer, syngeneic animal models of HNSCC, animal models of

- transplanted xenogeneic human tumors. *Int J Cancer*. (2006) 118:2111–22. doi: 10.1002/ijc.21694
26. Ballegeer EA, Madrill NJ, Berger KL, Agnew DW, McNeil EA. Evaluation of hypoxia in a feline model of head and neck cancer using (6)(4)Cu-ATSM positron emission tomography/computed tomography. *BMC Cancer*. (2013) 13:218. doi: 10.1186/1471-2407-13-218
 27. Rathore K, Alexander M, Cekanova M. Piroxicam inhibits Masitinib-induced cyclooxygenase 2 expression in oral squamous cell carcinoma cells *in vitro*. *Transl Res*. (2014) 164:158–68. doi: 10.1016/j.trsl.2014.02.002
 28. Supsavhad W, Dirksen WP, Martin CK, Rosol TJ. Animal models of head and neck squamous cell carcinoma. *Vet J*. (2016) 210:7–16. doi: 10.1016/j.tvjl.2015.11.006
 29. Frese KK, Tuveson DA. Maximizing mouse cancer models. *Nat Rev Cancer*. (2007) 7:645–58. doi: 10.1038/nrc2192
 30. Neville BW, Day TA. Oral cancer and precancerous lesions. *CA Cancer J Clin*. (2002) 52:195–215. doi: 10.3322/canjclin.52.4.195
 31. Johnson N. Tobacco use and oral cancer: a global perspective. *J Dental Educat*. (2001) 65:328–39. Available online at: <http://www.jdentaled.org/content/65/4/328.long>
 32. Hecht SS. Tobacco carcinogens, their biomarkers and tobacco-induced cancer. *Nat Rev Cancer*. (2003) 3:733–44. doi: 10.1038/nrc1190
 33. Jin F, Thaiparambil J, Donepudi SR, Vantaku V, Piyarathna DWB, Maity S, et al. Tobacco-specific carcinogens induce hypermethylation, DNA adducts, and DNA damage in bladder cancer. *Cancer Prev Res*. (2017) 10:588–97. doi: 10.1158/1940-6207.CAPR-17-0198
 34. Ludwig S, Hong CS, Razzo BM, Fabian KPL, Chelvanambi M, Lang S, et al. Impact of combination immunochemotherapies on progression of 4NQO-induced murine oral squamous cell carcinoma. *Cancer Immunol Immunother*. (2019) 68:1133–41. doi: 10.1007/s00262-019-02348-2
 35. Culp SJ, Gaylor DW, Sheldon WG, Goldstein LS, Beland FA. A comparison of the tumors induced by coal tar and benzo[a]pyrene in a 2-year bioassay. *Carcinogenesis*. (1998) 19:117–24. doi: 10.1093/carcin/19.1.117
 36. Guttenplan JB, Kosinska W, Zhao ZL, Chen KM, Aliaga C, DelTondo J, et al. Mutagenesis and carcinogenesis induced by dibenzo[a,l]pyrene in the mouse oral cavity: a potential new model for oral cancer. *Int J Cancer*. (2012) 130:2783–90. doi: 10.1002/ijc.26344
 37. Guttenplan JB, Chen KM, Sun YW, Shalaby NAE, Kosinska W, Desai D, et al. The effects of the tobacco carcinogens N²-nitrosornicotine and dibenzo[a,l]pyrene individually and in combination on DNA damage in human oral leukoplakia and on mutagenicity, and mutation profiles in lacI mouse tongue. *Chem Res Toxicol*. (2019) 32:1893–9. doi: 10.1021/acs.chemrestox.9b00257
 38. Chang NW, Pei RJ, Tseng HC, Yeh KT, Chan HC, Lee MR, et al. Co-treating with arecoline and 4-nitroquinoline 1-oxide to establish a mouse model mimicking oral tumorigenesis. *Chem Biol Interact*. (2010) 183:231–7. doi: 10.1016/j.cbi.2009.10.005
 39. Guo Y, Wang X, Zhang X, Sun Z, Chen X. Ethanol promotes chemically induced oral cancer in mice through activation of the 5-lipoxygenase pathway of arachidonic acid metabolism. *Cancer Prev Res*. (2011) 4:1863–72. doi: 10.1158/1940-6207.CAPR-11-0206
 40. Kanojia D, Vaidya MM. 4-nitroquinoline-1-oxide induced experimental oral carcinogenesis. *Oral Oncol*. (2006) 42:655–67. doi: 10.1016/j.oraloncology.2005.10.013
 41. Kartasova T, Cornelissen BJ, Belt P, van de Putte P. Effects of UV, 4-NQO and TPA on gene expression in cultured human epidermal keratinocytes. *Nucleic Acids Res*. (1987) 15:5945–62. doi: 10.1093/nar/15.15.5945
 42. Kondo S. A test for mutation theory of cancer: carcinogenesis by misrepair of DNA damaged by 4-nitroquinoline 1-oxide. *Br J Cancer*. (1977) 35:595–601. doi: 10.1038/bjc.1977.93
 43. Kao YY, Tu HF, Kao SY, Chang KW, Lin SC. The increase of oncogenic miRNA expression in tongue carcinogenesis of a mouse model. *Oral Oncol*. (2015) 51:1103–12. doi: 10.1016/j.oraloncology.2015.10.007
 44. Koike R, Uchiyama T, Arimoto-Kobayashi S, Okamoto K, Negishi T. Increase of somatic cell mutations in oxidative-damage-sensitive drosophila. *Genes Environ*. (2018) 40:3. doi: 10.1186/s41021-017-0090-z
 45. Arima Y, Nishigori C, Takeuchi T, Oka S, Morimoto K, Utani A, et al. 4-Nitroquinoline 1-oxide forms 8-hydroxydeoxyguanosine in human fibroblasts through reactive oxygen species. *Toxicol Sci*. (2006) 91:382–92. doi: 10.1093/toxsci/kfj161
 46. Moloney JN, Cotter TG. ROS signalling in the biology of cancer. *Semin Cell Dev Biol*. (2018) 80:50–64. doi: 10.1016/j.semcdb.2017.05.023
 47. Yang J, Zhao X, Tang M, Li L, Lei Y, Cheng P, et al. The role of ROS and subsequent DNA-damage response in PUMA-induced apoptosis of ovarian cancer cells. *Oncotarget*. (2017) 8:23492–506. doi: 10.18632/oncotarget.15626
 48. Tsai CH, Hung AC, Chen YY, Chiu YW, Hsieh PW, Lee YC, et al. 3'-hydroxy-4'-methoxy- β -methyl- β -nitrostyrene inhibits tumorigenesis in colorectal cancer cells through ROS-mediated DNA damage and mitochondrial dysfunction. *Oncotarget*. (2017) 8:18106–17. doi: 10.18632/oncotarget.14996
 49. El-Hussein A, Hamblin MR. ROS generation and DNA damage with photoinactivation mediated by silver nanoparticles in lung cancer cell line. *IET Nanobiotechnol*. (2017) 11:173–8. doi: 10.1049/iet-nbt.2015.0083
 50. Benson AM. Conversion of 4-nitroquinoline 1-oxide. (4NQO) to 4-hydroxyaminoquinoline 1-oxide by a dicumarol-resistant hepatic 4NQO nitroreductase in rats and mice. *Biochem Pharmacol*. (1993) 46:1217–21. doi: 10.1016/0006-2952(93)90470-H
 51. Friedberg EC. A history of the DNA repair and mutagenesis field: I. The discovery of enzymatic photoreactivation. *DNA Repair (Amst)*. (2015) 33:35–42. doi: 10.1016/j.dnarep.2015.06.007
 52. Morrow CS, Diah S, Smitherman PK, Schneider E, Townsend AJ. Multidrug resistance protein and glutathione S-transferase P1–1 act in synergy to confer protection from 4-nitroquinoline 1-oxide toxicity. *Carcinogenesis*. (1998) 19:109–15. doi: 10.1093/carcin/19.1.109
 53. Tada M, Tada M. Main binding sites of the carcinogen, 4-nitroquinoline 1-oxide in nucleic acids. *Biochim Biophys Acta*. (1976) 454:558–66. doi: 10.1016/0005-2787(76)90281-1
 54. Winkle SA, Tinoco I Jr. Interactions of 4-nitroquinoline 1-oxide with four deoxyribonucleotides. *Biochemistry*. (1978) 17:1352–6. doi: 10.1021/bi00600a033
 55. Galiegue-Zouitina S, Bailleul B, Loucheux-Lefebvre MH. Adducts from *in vivo* action of the carcinogen 4-hydroxyaminoquinoline 1-oxide in rats and from *in vitro* reaction of 4-acetoxyaminoquinoline 1-oxide with DNA and polynucleotides. *Cancer Res*. (1985) 45:520–5.
 56. Fronza G, Campomenosi P, Iannone R, Abbondandolo A. The 4-nitroquinoline 1-oxide mutational spectrum in single stranded DNA is characterized by guanine to pyrimidine transversions. *Nucleic Acids Res*. (1992) 20:1283–7. doi: 10.1093/nar/20.6.1283
 57. Galiegue-Zouitina S, Daubersies P, Loucheux-Lefebvre MH, Bailleul B. Mutagenicity of N² guanylation is SOS functions dependent and reminiscent of the high mutagenic property of 4NQO. *Carcinogenesis*. (1989) 10:1961–6. doi: 10.1093/carcin/10.10.1961
 58. Li J, Liang F, Yu D, Qing H, Yang Y. Development of a 4-nitroquinoline-1-oxide model of lymph node metastasis in oral squamous cell carcinoma. *Oral Oncol*. (2013) 49:299–305. doi: 10.1016/j.oraloncology.2012.10.013
 59. Tang XH, Osei-Sarfo K, Urvalek AM, Zhang T, Scognamiglio T, Gudas LJ. Combination of beaxotene and the retinoid CD1530 reduces murine oral-cavity carcinogenesis induced by the carcinogen 4-nitroquinoline 1-oxide. *Proc Natl Acad Sci USA*. (2014) 111:8907–12. doi: 10.1073/pnas.1404828111
 60. Lu G, Wang D, Qin X, Muller S, Wang X, Chen AY, et al. Detection and delineation of squamous neoplasia with hyperspectral imaging in a mouse model of tongue carcinogenesis. *J Biophoton*. (2018) 11:e201700078. doi: 10.1002/jbio.201700078
 61. Scheff NN, Ye Y, Bhattacharya A, MacRae J, Hickman DN, Sharma AK, et al. Tumor necrosis factor alpha secreted from oral squamous cell carcinoma contributes to cancer pain and associated inflammation. *Pain*. (2017) 158:2396–409. doi: 10.1097/j.pain.0000000000001044
 62. Ye Y, Ono K, Bernabe DG, Viet CT, Pickering V, Dolan JC, et al. Adenosine triphosphate drives head and neck cancer pain through P2X2/3 heterotrimers. *Acta Neuropathol Commun*. (2014) 2:62. doi: 10.1186/2051-5960-2-62
 63. Yuan B, Oechsli MN, Hendler FJ. A region within murine chromosome 7F4, syntenic to the human 11q13 amplicon, is frequently amplified in 4NQO-induced oral cavity tumors. *Oncogene*. (1997) 15:1161–70. doi: 10.1038/sj.onc.1201269

64. Liu H, Li J, Yang Y, Liu L, Yu L, Tu M, et al. Alterations of 63 hub genes during lingual carcinogenesis in C57BL/6J mice. *Sci Rep.* (2018) 8:12626. doi: 10.1038/s41598-018-31103-3
65. Schoop RA, Noteborn MH, Baatenburg de Jong RJ. A mouse model for oral squamous cell carcinoma. *J Mol Histol.* (2009) 40:177–81. doi: 10.1007/s10735-009-9228-z
66. Booth DR. A relationship found between intra-oral sites of 4NQO reductase activity and chemical carcinogenesis. *Cell Tissue Kinet.* (1990) 23:331–40. doi: 10.1111/j.1365-2184.1990.tb01129.x
67. Tang XH, Knudsen B, Bemis D, Tickoo S, Gudas LJ. Oral cavity and esophageal carcinogenesis modeled in carcinogen-treated mice. *Clin Cancer Res.* (2004) 10:301–13. doi: 10.1158/1078-0432.CCR-0999-3
68. Vered M, Yarom N, Dayan D. 4NQO oral carcinogenesis: animal models, molecular markers and future expectations. *Oral Oncol.* (2005) 41:337–9. doi: 10.1016/j.oraloncology.2004.07.005
69. Hasina R, Mollberg N, Kawada I, Mutreja K, Kanade G, Yala S, et al. Critical role for the receptor tyrosine kinase EPHB4 in esophageal cancers. *Cancer Res.* (2013) 73:184–94. doi: 10.1158/0008-5472.CAN-12-0915
70. Maji S, Samal SK, Pattanaik L, Panda S, Quinn BA, Das SK, et al. Mcl-1 is an important therapeutic target for oral squamous cell carcinomas. *Oncotarget.* (2015) 6:16623–37. doi: 10.18632/oncotarget.3932
71. Jiang L, Huang R, Wu Y, Diao P, Zhang W, Li J, et al. Overexpression of CDK7 is associated with unfavourable prognosis in oral squamous cell carcinoma. *Pathology.* (2019) 51:74–80. doi: 10.1016/j.pathol.2018.10.004
72. Droguett D, Castillo C, Leiva E, Theoduloz C, Schmeda-Hirschmann G, Kemmerling U. Efficacy of quercetin against chemically induced murine oral squamous cell carcinoma. *Oncol Lett.* (2015) 10:2432–8. doi: 10.3892/ol.2015.3598
73. Foy JP, Tortoreau A, Caulin C, Le Texier V, Lavergne E, Thomas E, et al. The dynamics of gene expression changes in a mouse model of oral tumorigenesis may help refine prevention and treatment strategies in patients with oral cancer. *Oncotarget.* (2016) 7:35932–45. doi: 10.18632/oncotarget.8321
74. Wu JS, Zheng M, Zhang M, Pang X, Li L, Wang SS, et al. *Porphyromonas gingivalis* promotes 4-nitroquinoline-1-oxide-induced oral carcinogenesis with an alteration of fatty acid metabolism. *Front Microbiol.* (2018) 9:2081. doi: 10.3389/fmicb.2018.02081
75. Liu YC, Ho HC, Lee MR, Yeh CM, Tseng HC, Lin YC, et al. Cortactin is a prognostic marker for oral squamous cell carcinoma and its overexpression is involved in oral carcinogenesis. *Environ Toxicol.* (2017) 32:799–812. doi: 10.1002/tox.22280
76. Vincent-Chong VK, DeJong H, Rich LJ, Patti A, Merzianu M, Hershberger PA, et al. Impact of age on disease progression and microenvironment in oral cancer. *J Dent Res.* (2018) 97:1268–76. doi: 10.1177/0022034518775736
77. Vitale-Cross L, Czerninski R, Amornphimoltham P, Patel V, Molinolo AA, Gutkind JS. Chemical carcinogenesis models for evaluating molecular-targeted prevention and treatment of oral cancer. *Cancer Prev Res.* (2009) 2:419–22. doi: 10.1158/1940-6207.CAPR-09-0058
78. Bisetto S, Whitaker-Menezes D, Wilski NA, Tuluc M, Curry J, Zhan T, et al. Monocarboxylate transporter 4 (MCT4) knockout mice have attenuated 4NQO induced carcinogenesis; a role for MCT4 in driving oral squamous cell cancer. *Front Oncol.* (2018) 8:324. doi: 10.3389/fonc.2018.00324
79. Chen Y, Jiang Y, Liao L, Zhu X, Tang S, Yang Q, et al. Inhibition of 4NQO-induced oral carcinogenesis by dietary oyster shell calcium. *Integr Cancer Ther.* (2016) 15:96–101. doi: 10.1177/1534735415596572
80. Fujino H, Chino T, Imai T. Experimental production of labial and lingual carcinoma by local application of 4-nitroquinoline N-oxide. *J Natl Cancer Inst.* (1965) 35:907–18.
81. Khandelwal AR, Moore-Medlin T, Ekshyyan O, Gu X, Abreo F, Nathan CO. Local and systemic curcumin C3 complex inhibits 4NQO-induced oral tumorigenesis via modulating FGF-2/FGFR-2 activation. *Am J Cancer Res.* (2018) 8:2538–47.
82. Tamura T, Ichikawa T, Nakahata S, Kondo Y, Tagawa Y, Yamamoto K, et al. Loss of NDRG2 expression confers oral squamous cell carcinoma with enhanced metastatic potential. *Cancer Res.* (2017) 77:2363–74. doi: 10.1158/0008-5472.CAN-16-2114
83. Wu T, Hong Y, Jia L, Wu J, Xia J, Wang J, et al. Modulation of IL-1 β reprogrammes the tumor microenvironment to interrupt oral carcinogenesis. *Sci Rep.* (2016) 6:20208. doi: 10.1038/srep20208
84. Chen Y, Wang X, Fang J, Song J, Ma D, Luo L, et al. Mesenchymal stem cells participate in oral mucosa carcinogenesis by regulating T cell proliferation. *Clin Immunol.* (2019) 198:46–53. doi: 10.1016/j.clim.2018.12.001
85. Young MR. Use of carcinogen-induced premalignant oral lesions in a dendritic cell-based vaccine to stimulate immune reactivity against both premalignant oral lesions and oral cancer. *J Immunother.* (2008) 31:148–56. doi: 10.1097/CJI.0b013e31815b5dbf5
86. Li J, Qiu G, Fang B, Dai X, Cai J. Deficiency of IL-18 aggravates esophageal carcinoma through inhibiting IFN- γ production by CD8(+)T cells and NK cells. *Inflammation.* (2018) 41:667–76. doi: 10.1007/s10753-017-0721-3
87. Ludwig N, Yermeni SS, Razzo BM, Whiteside TL. Exosomes from HNSCC promote angiogenesis through reprogramming of endothelial cells. *Mol Cancer Res.* (2018) 16:1798–808. doi: 10.1158/1541-7786.MCR-18-0358
88. Ohnishi Y, Fujii T, Ugaki Y, Yasui H, Watanabe M, Dateoka S, et al. Usefulness of a fluorescence visualization system for the detection of oral precancerous and early cancerous lesions. *Oncol Rep.* (2016) 36:514–20. doi: 10.3892/or.2016.4776
89. Wang J, Xie T, Wang B, William WN Jr, Heymach JV, El-Naggar AK, et al. PD-1 Blockade prevents the development and progression of carcinogen-induced oral premalignant lesions. *Cancer Prev Res.* (2017) 10:684–93. doi: 10.1158/1940-6207.CAPR-17-0108
90. Chen Y, Li Q, Li X, Ma D, Fang J, Luo L, et al. Blockade of PD-1 effectively inhibits in vivo malignant transformation of oral mucosa. *Oncimmunology.* (2018) 7:e1388484. doi: 10.1080/2162402X.2017.1388484
91. Chu M, Su YX, Wang L, Zhang TH, Liang YJ, Liang LZ, et al. Myeloid-derived suppressor cells contribute to oral cancer progression in 4NQO-treated mice. *Oral Dis.* (2012) 18:67–73. doi: 10.1111/j.1601-0825.2011.01846.x
92. Chen WC, Lai CH, Chuang HC, Lin PY, Chen MF. Inflammation-induced myeloid-derived suppressor cells associated with squamous cell carcinoma of the head and neck. *Head Neck.* (2017) 39:347–55. doi: 10.1002/hed.24595
93. Oghumu S, Knobloch TJ, Terrazas C, Varikuti S, Ahn-Jarvis J, Bollinger CE, et al. Deletion of macrophage migration inhibitory factor inhibits murine oral carcinogenesis: Potential role for chronic pro-inflammatory immune mediators. *Int J Cancer.* (2016) 139:1379–90. doi: 10.1002/ijc.30177
94. Wu JS, Li L, Wang SS, Pang X, Wu JB, Sheng SR, et al. Autophagy is positively associated with the accumulation of myeloid-derived suppressor cells in 4-nitroquinoline-1-oxide-induced oral cancer. *Oncol Rep.* (2018) 40:3381–91. doi: 10.3892/or.2018.6747
95. Wen L, Lu H, Li Q, Li Q, Wen S, Wang D, et al. Contributions of T cell dysfunction to the resistance against anti-PD-1 therapy in oral carcinogenesis. *J Exp Clin Cancer Res.* (2019) 38:299. doi: 10.1186/s13046-019-1185-0
96. De Costa AM, Justis DN, Schuyler CA, Young MR. Administration of a vaccine composed of dendritic cells pulsed with premalignant oral lesion lysate to mice bearing carcinogen-induced premalignant oral lesions stimulates a protective immune response. *Int Immunopharmacol.* (2012) 13:322–30. doi: 10.1016/j.intimp.2012.05.004
97. Phillips DH. Polycyclic aromatic hydrocarbons in the diet. *Mutat Res.* (1999) 443:139–47. doi: 10.1016/S1383-5742(99)00016-2
98. Prahalad AK, Ross JA, Nelson GB, Roop BC, King LC, Nesnow S, et al. Dibenzo[a,l]pyrene-induced DNA adduction, tumorigenicity, and Ki-ras oncogene mutations in strain A/J mouse lung. *Carcinogenesis.* (1997) 18:1955–63. doi: 10.1093/carcin/18.10.1955
99. Cavalieri EL, Rogan EG, Higginbotham S, Cremonesi P, Salmasi S. Tumor-initiating activity in mouse skin and carcinogenicity in rat mammary gland of dibenzo[a,l]pyrenes: the very potent environmental carcinogen dibenzo[a,l]pyrene. *J Cancer Res Clin Oncol.* (1989) 115:67–72. doi: 10.1007/BF00391602
100. Higginbotham S, RamaKrishna NV, Johansson SL, Rogan EG, Cavalieri EL. Tumor-initiating activity and carcinogenicity of dibenzo[a,l]pyrene versus 7,12-dimethylbenz[a]anthracene and benzo[a]pyrene at low doses in mouse skin. *Carcinogenesis.* (1993) 14:875–8. doi: 10.1093/carcin/14.5.875

101. Tu HF, Chen MY, Lai JC, Chen YL, Wong YW, Yang CC, et al. Arecoline-regulated ataxia telangiectasia mutated expression level in oral cancer progression. *Head Neck*. (2019) 41:2525–37. doi: 10.1002/hed.25718
102. Kuo TM, Nithiyantham S, Lee CP, Hsu HT, Luo SY, Lin YZ, et al. Arecoline N-oxide regulates oral squamous cell carcinoma development through NOTCH1 and FAT1 expressions. *J Cell Physiol*. (2019) 234:13984–93. doi: 10.1002/jcp.28084
103. Lo WY, Tsai MH, Tsai Y, Hua CH, Tsai FJ, Huang SY, et al. Identification of over-expressed proteins in oral squamous cell carcinoma. (OSCC) patients by clinical proteomic analysis. *Clin Chim Acta*. (2007) 376:101–7. doi: 10.1016/j.cca.2006.06.030
104. Rygaard J, Povlsen CO. Heterotransplantation of a human malignant tumour to “Nude” mice. *Acta Pathol Microbiol Scand*. (1969) 77:758–60. doi: 10.1111/j.1699-0463.1969.tb04520.x
105. Sikder H, Huso DL, Zhang H, Wang B, Ryu B, Hwang ST, et al. Disruption of Id1 reveals major differences in angiogenesis between transplanted and autochthonous tumors. *Cancer Cell*. (2003) 4:291–9. doi: 10.1016/S1535-6108(03)00245-9
106. Lwin TM, Hoffman RM, Bouvet M. Advantages of patient-derived orthotopic mouse models and genetic reporters for developing fluorescence-guided surgery. *J Surg Oncol*. (2018) 118:253–64. doi: 10.1002/jso.25150
107. Chodroff L, Bendele M, Valenzuela V, Henry M, Ruparel S. EXPRESS: BDNF signaling contributes to oral cancer pain in a preclinical orthotopic rodent model. *Mol Pain*. (2016) 12:1–17. doi: 10.1177/1744806916666841
108. Johnson JI, Decker S, Zaharevitz D, Rubinstein LV, Venditti JM, Schepartz S, et al. Relationships between drug activity in NCI preclinical *in vitro* and *in vivo* models and early clinical trials. *Br J Cancer*. (2001) 84:1424–31. doi: 10.1054/bjoc.2001.1796
109. Ledford H. US cancer institute to overhaul tumour cell lines. *Nature*. (2016) 530:391. doi: 10.1038/nature.2016.19364
110. Dong Y, Zhao Q, Ma X, Ma G, Liu C, Chen Z, et al. Establishment of a new OSCC cell line derived from OLK and identification of malignant transformation-related proteins by differential proteomics approach. *Sci Rep*. (2015) 5:12668. doi: 10.1038/srep12668
111. Rivera C, Zandonadi FS, Sanchez-Romero C, Soares CD, Granato DC, Gonzalez-Arriagada WA, et al. Agrin has a pathological role in the progression of oral cancer. *Br J Cancer*. (2018) 118:1628–38. doi: 10.1038/s41416-018-0135-5
112. Sun S, Zhang Z. Patient-derived xenograft platform of OSCC: a renewable human bio-bank for preclinical cancer research and a new co-clinical model for treatment optimization. *Front Med*. (2016) 10:104–10. doi: 10.1007/s11684-016-0432-4
113. Maykel J, Liu JH, Li H, Shultz LD, Greiner DL, Houghton J. NOD-scidIl2rg. (tm1Wjl) and NOD-Rag1. (null) Il2rg. (tm1Wjl): a model for stromal cell-tumor cell interaction for human colon cancer. *Digest Dis Sci*. (2014) 59:1169–79. doi: 10.1007/s10620-014-3168-5
114. Sumareva R, Ukrainsky G, Kiremidjian-Schumacher L, Roy M, Wishe HI, Steinfeld AD, et al. Effect of combined adoptive immunotherapy and radiotherapy on tumor growth. *Radiation Oncol Invest*. (1999) 7:22–9. doi: 10.1002/(SICI)1520-6823(1999)7:1<22::AID-ROI3>3.0.CO;2-6
115. Mery B, Rancoule C, Guy JB, Espenel S, Wozny AS, Battiston-Montagne P, et al. Preclinical models in HNSCC: a comprehensive review. *Oral Oncol*. (2017) 65:51–6. doi: 10.1016/j.oraloncology.2016.12.010
116. Fitch KA. The development of a head and neck tumor model in the nude mouse. *Head Neck Oncol Res*. (1988) 187–90.
117. Myers JN, Holsinger FC, Jasser SA, Bekele BN, Fidler IJ. An orthotopic nude mouse model of oral tongue squamous cell carcinoma. *Clin Cancer Res*. (2002) 8:293–8. Available online at: <https://clincancerres.aacrjournals.org/content/8/1/293.long>
118. Agliano A, Martin-Padura I, Mancuso P, Marighetti P, Rabascio C, Pruneri G, et al. Human acute leukemia cells injected in NOD/LtSz-scid/IL-2Rgamma null mice generate a faster and more efficient disease compared to other NOD/scid-related strains. *Int J Cancer*. (2008) 123:2222–7. doi: 10.1002/ijc.23772
119. Takenaka K, Prasolava TK, Wang JC, Mortin-Toth SM, Khalouei S, Gan OI, et al. Polymorphism in Sirpa modulates engraftment of human hematopoietic stem cells. *Nat Immunol*. (2007) 8:1313–23. doi: 10.1038/ni1527
120. Phillips RA, Jewett MA, Gallie BL. Growth of human tumors in immune-deficient scid mice and nude mice. *Curr Top Microbiol Immunol*. (1989) 152:259–63. doi: 10.1007/978-3-642-74974-2_31
121. Szadvari I, Krizanova O, Babula P. Athymic nude mice as an experimental model for cancer treatment. *Physiol Res*. (2016) 65(Suppl 4):S441–S53. Available online at: http://www.biomed.cas.cz/physiolres/pdf/65/65_S441.pdf
122. Bosma MJ, Carroll AM. The SCID mouse mutant: definition, characterization, and potential uses. *Annual Rev Immunol*. (1991) 9:323–50. doi: 10.1146/annurev.iy.09.040191.001543
123. Prochazka M, Gaskins HR, Shultz LD, Leiter EH. The nonobese diabetic scid mouse: model for spontaneous thymomagenesis associated with immunodeficiency. *Proc Natl Acad Sci USA*. (1992) 89:3290–4. doi: 10.1073/pnas.89.8.3290
124. Ito M, Hiramatsu H, Kobayashi K, Suzue K, Kawahata M, Hioki K, et al. NOD/SCID/gamma(c)(null) mouse: an excellent recipient mouse model for engraftment of human cells. *Blood*. (2002) 100:3175–82. doi: 10.1182/blood-2001-12-0207
125. Shultz LD, Lyons BL, Burzenski LM, Gott B, Chen X, Chaleff S, et al. Human lymphoid and myeloid cell development in NOD/LtSz-scid IL2R gamma null mice engrafted with mobilized human hemopoietic stem cells. *J Immunol*. (2005) 174:6477–89. doi: 10.4049/jimmunol.174.10.6477
126. Dinesman A, Haughey B, Gates GA, Aufdemorte T, Von Hoff DD. Development of a new *in vivo* model for head and neck cancer. *Otolaryngol Head Neck Surg*. (1990) 103:766–74. doi: 10.1177/019459989010300517
127. Behren A, Kamenisch Y, Muehlen S, Flechtenmacher C, Haberkorn U, Hilber H, et al. Development of an oral cancer recurrence mouse model after surgical resection. *Int J Oncol*. (2010) 36:849–55. doi: 10.3892/ijo.00000562
128. Roh V, Abramowski P, Hiou-Feige A, Cornils K, Rivals JP, Zougman A, et al. Cellular barcoding identifies clonal substitution as a hallmark of local recurrence in a surgical model of head and neck squamous cell carcinoma. *Cell Rep*. (2018) 25:2208–22.e7. doi: 10.1016/j.celrep.2018.10.090
129. Li J, Huang J, Jeong JH, Park SJ, Wei R, Peng J, et al. Selective TBK1/IKK dual inhibitors with anticancer potency. *Int J Cancer*. (2014) 134:1972–80. doi: 10.1002/ijc.28507
130. Brand TM, Hartmann S, Bholra NE, Li H, Zeng Y, O’Keefe RA, et al. Crosstalk Signaling between HER3 and HPV16 E6 and E7 mediates resistance to PI3K inhibitors in head and neck cancer. *Cancer Res*. (2018) 78:2383–95. doi: 10.1158/0008-5472.CAN-17-1672
131. Bais MV, Kukuruzinska M, Trackman PC. Orthotopic non-metastatic and metastatic oral cancer mouse models. *Oral Oncol*. (2015) 51:476–82. doi: 10.1016/j.oraloncology.2015.01.012
132. Pearson AT, Finkel KA, Warner KA, Nor F, Tice D, Martins MD, et al. Patient-derived xenograft. (PDX) tumors increase growth rate with time. *Oncotarget*. (2016) 7:7993–8005. doi: 10.18632/oncotarget.6919
133. Li H, Wheeler S, Park Y, Ju Z, Thomas SM, Fichera M, et al. Proteomic characterization of head and neck cancer patient-derived xenografts. *Mol Cancer Res*. (2016) 14:278–86. doi: 10.1158/1541-7786.MCR-15-0354
134. Bothwell KD, Shaurova T, Merzianu M, Suresh A, Kuriakose MA, Johnson CS, et al. Impact of short-term 1,25-dihydroxyvitamin D3 on the chemopreventive efficacy of erlotinib against oral cancer. *Cancer Prev Res*. (2015) 8:765–76. doi: 10.1158/1940-6207.CAPR-14-0454
135. Seshadri M, Merzianu M, Tang H, Rigual NR, Sullivan M, Loree TR, et al. Establishment and characterization of patient tumor-derived head and neck squamous cell carcinoma xenografts. *Cancer Biol Ther*. (2009) 8:2275–83. doi: 10.4161/cbt.8.23.10137
136. Lu Z, He Q, Liang J, Li W, Su Q, Chen Z, et al. miR-31–5p Is a potential circulating biomarker and therapeutic target for oral cancer. *Mol Ther Nucleic Acids*. (2019) 16:471–80. doi: 10.1016/j.omtn.2019.03.012
137. Kerk SA, Finkel KA, Pearson AT, Warner KA, Zhang Z, Nor F, et al. 5T4-targeted therapy ablates cancer stem cells and prevents recurrence of head and neck squamous cell carcinoma. *Clin Cancer Res*. (2017) 23:2516–27. doi: 10.1158/1078-0432.CCR-16-1834
138. Rich LJ, Seshadri M. Photoacoustic monitoring of tumor and normal tissue response to radiation. *Sci Rep*. (2016) 6:21237. doi: 10.1038/srep21237
139. Zhang L, Nomie K, Zhang H, Bell T, Pham L, Kadri S, et al. B-cell lymphoma patient-derived xenograft models enable drug discovery and

- are a platform for personalized therapy. *Clin Cancer Res.* (2017) 23:4212–23. doi: 10.1158/1078-0432.CCR-16-2703
140. Fang Z, Zhao J, Xie W, Sun Q, Wang H, Qiao B. LncRNA UCA1 promotes proliferation and cisplatin resistance of oral squamous cell carcinoma by suppressing miR-184 expression. *Cancer Med.* (2017) 6:2897–908. doi: 10.1002/cam4.1253
 141. Feng X, Luo Q, Zhang H, Wang H, Chen W, Meng G, et al. The role of NLRP3 inflammasome in 5-fluorouracil resistance of oral squamous cell carcinoma. *J Exp Clin Cancer Res.* (2017) 36:81. doi: 10.1186/s13046-017-0553-x
 142. Ozawa H, Ranaweera RS, Izumchenko E, Makarev E, Zhavoronkov A, Fertig EJ, et al. SMAD4 loss is associated with cetuximab resistance and induction of MAPK/JNK activation in head and neck cancer cells. *Clin Cancer Res.* (2017) 23:5162–75. doi: 10.1158/1078-0432.CCR-16-1686
 143. Ma J, Ren Y, Zhang L, Kong X, Wang T, Shi Y, et al. Knocking-down of CREPT prohibits the progression of oral squamous cell carcinoma and suppresses cyclin D1 and c-Myc expression. *PLoS ONE.* (2017) 12:e0174309. doi: 10.1371/journal.pone.0174309
 144. Wang Y, Zhu Y, Wang Q, Hu H, Li Z, Wang D, et al. The histone demethylase LSD1 is a novel oncogene and therapeutic target in oral cancer. *Cancer Lett.* (2016) 374:12–21. doi: 10.1016/j.canlet.2016.02.004
 145. Tohyama R, Kayamori K, Sato K, Hamagaki M, Sakamoto K, Yasuda H, et al. Establishment of a xenograft model to explore the mechanism of bone destruction by human oral cancers and its application to analysis of role of RANKL. *J Oral Pathol Med.* (2016) 45:356–64. doi: 10.1111/jop.12376
 146. Wang Y, Guo W, Li Z, Wu Y, Jing C, Ren Y, et al. Role of the EZH2/miR-200 axis in STAT3-mediated OSCC invasion. *Int J Oncol.* (2018) 52:1149–64. doi: 10.3892/ijo.2018.4293
 147. Wang H, Luo Q, Feng X, Zhang R, Li J, Chen F. NLRP3 promotes tumor growth and metastasis in human oral squamous cell carcinoma. *BMC Cancer.* (2018) 18:500. doi: 10.1186/s12885-018-4403-9
 148. Jia L, Wang J, Wu T, Wu J, Ling J, Cheng B. *In vitro* and *in vivo* antitumor effects of chloroquine on oral squamous cell carcinoma. *Mol Med Rep.* (2017) 16:5779–86. doi: 10.3892/mmr.2017.7342
 149. Sasabe E, Tomomura A, Tomita R, Sento S, Kitamura N, Yamamoto T. Ephrin-B2 reverse signaling regulates progression and lymph node metastasis of oral squamous cell carcinoma. *PLoS ONE.* (2017) 12:e0188965. doi: 10.1371/journal.pone.0188965
 150. Campbell KM, Lin T, Zolkind P, Barnell EK, Skidmore ZL, Winkler AE, et al. Oral cavity squamous cell carcinoma xenografts retain complex genotypes and intertumor molecular heterogeneity. *Cell Rep.* (2018) 24:2167–78. doi: 10.1016/j.celrep.2018.07.058
 151. Su H, Luo Q, Xie H, Huang X, Ni Y, Mou Y, et al. Therapeutic antitumor efficacy of tumor-derived autophagosome. (DRibble) vaccine on head and neck cancer. *Int J Nanomed.* (2015) 10:1921–30. doi: 10.2147/IJN.S74204
 152. Dong H, Su H, Chen L, Liu K, Hu HM, Yang W, et al. Immunocompetence and mechanism of the DRibble-DCs vaccine for oral squamous cell carcinoma. *Cancer Manage Res.* (2018) 10:493–501. doi: 10.2147/CMAR.S155914
 153. Nagaya T, Nakamura Y, Okuyama S, Ogata F, Maruoka Y, Choyke PL, et al. Syngeneic mouse models of oral cancer are effectively targeted by anti-CD44-based NIR-PIT. *Mol Cancer Res.* (2017) 15:1667–77. doi: 10.1158/1541-7786.MCR-17-0333
 154. Chung MK, Jung YH, Lee JK, Cho SY, Murillo-Sauca O, Uppaluri R, et al. CD271 confers an invasive and metastatic phenotype of head and neck squamous cell carcinoma through the upregulation of slug. *Clin Cancer Res.* (2018) 24:674–83. doi: 10.1158/1078-0432.CCR-17-0866
 155. Judd NP, Allen CT, Winkler AE, Uppaluri R. Comparative analysis of tumor-infiltrating lymphocytes in a syngeneic mouse model of oral cancer. *Otolaryngol Head Neck Surg.* (2012) 147:493–500. doi: 10.1177/0194599812442037
 156. Adachi M, Mizuno-Kamiya M, Takayama E, Kawaki H, Inagaki T, Sumi S, et al. Gene expression analyses associated with malignant phenotypes of metastatic sub-clones derived from a mouse oral squamous cell carcinoma Sq-1979 cell line. *Oncol Lett.* (2018) 15:3350–6. doi: 10.3892/ol.2017.7648
 157. Moroishi T, Hayashi T, Pan WW, Fujita Y, Holt MV, Qin J, et al. The hippo pathway kinases LATS1/2 suppress cancer immunity. *Cell.* (2016) 167:1525–39e17. doi: 10.1016/j.cell.2016.11.005
 158. Chen YF, Chang KW, Yang IT, Tu HF, Lin SC. Establishment of syngeneic murine model for oral cancer therapy. *Oral Oncol.* (2019) 95:194–201. doi: 10.1016/j.oraloncology.2019.06.026
 159. Chen YF, Liu CJ, Lin LH, Chou CH, Yeh LY, Lin SC, et al. Establishing of mouse oral carcinoma cell lines derived from transgenic mice and their use as syngeneic tumorigenesis models. *BMC Cancer.* (2019) 19:281. doi: 10.1186/s12885-019-5486-7
 160. De La Rochere P, Guil-Luna S, Decaudin D, Azar G, Sidhu SS, Piaggio E. Humanized mice for the study of immuno-oncology. *Trends Immunol.* (2018) 39:748–63. doi: 10.1016/j.it.2018.07.001
 161. Walsh NC, Kenney LL, Jangalwe S, Aryee KE, Greiner DL, Brehm MA, et al. Humanized mouse models of clinical disease. *Annu Rev Pathol.* (2017) 12:187–215. doi: 10.1146/annurev-pathol-052016-100332
 162. Morton JJ, Bird G, Keysar SB, Astling DP, Lyons TR, Anderson RT, et al. XactMice: humanizing mouse bone marrow enables microenvironment reconstitution in a patient-derived xenograft model of head and neck cancer. *Oncogene.* (2016) 35:290–300. doi: 10.1038/onc.2015.94
 163. Morton JJ, Keysar SB, Perrenoud L, Chimed TS, Reisinger J, Jackson B, et al. Dual use of hematopoietic and mesenchymal stem cells enhances engraftment and immune cell trafficking in an allogeneic humanized mouse model of head and neck cancer. *Mol Carcinog.* (2018) 57:1651–63. doi: 10.1002/mc.22887
 164. Morton JJ, Bird G, Refaeli Y, Jimeno A. Humanized mouse xenograft models: narrowing the tumor-microenvironment gap. *Cancer Res.* (2016) 76:6153–8. doi: 10.1158/0008-5472.CAN-16-1260
 165. Greenblatt MB, Vrbanc V, Tivey T, Tsang K, Tager AM, Aliprantis AO. Graft versus host disease in the bone marrow, liver and thymus humanized mouse model. *PLoS ONE.* (2012) 7:e44664. doi: 10.1371/journal.pone.0044664
 166. Sathish N, Wang X, Yuan Y. Human papillomavirus (HPV)-associated oral cancers and treatment strategies. *J Dental Res.* (2014) 93(7 Suppl):29–36s. doi: 10.1177/0022034514527969
 167. zur Hausen H. Papillomaviruses and cancer: from basic studies to clinical application. *Nat Rev Cancer.* (2002) 2:342–50. doi: 10.1038/nrc798
 168. Ghittoni R, Accardi R, Hasan U, Gheit T, Sylla B, Tommasino M. The biological properties of E6 and E7 oncoproteins from human papillomaviruses. *Virus Genes.* (2010) 40:1–13. doi: 10.1007/s11262-009-0412-8
 169. Brand TM, Hartmann S, Bhola NE, Peyser ND, Li H, Zeng Y, et al. Human papillomavirus regulates HER3 expression in head and neck cancer: implications for targeted HER3 therapy in HPV(+) patients. *Clin Cancer Res.* (2017) 23:3072–83. doi: 10.1158/1078-0432.CCR-16-2203
 170. Keysar SB, Astling DP, Anderson RT, Vogler BW, Bowles DW, Morton JJ, et al. A patient tumor transplant model of squamous cell cancer identifies PI3K inhibitors as candidate therapeutics in defined molecular bins. *Mol Oncol.* (2013) 7:776–90. doi: 10.1016/j.molonc.2013.03.004
 171. Facompre ND, Sahu V, Montone KT, Harmeyer KM, Nakagawa H, Rustgi AK, et al. Barriers to generating PDX models of HPV-related head and neck cancer. *Laryngoscope.* (2017) 127:2777–83. doi: 10.1002/lary.26679
 172. Taberna M, Mena M, Pavon MA, Alemany L, Gillison ML, Mesia R. Human papillomavirus-related oropharyngeal cancer. *Annal Oncol.* (2017) 28:2386–98. doi: 10.1093/annonc/mdx304
 173. Hoover AC, Spanos WC, Harris GF, Anderson ME, Klingelutz AJ, Lee JH. The role of human papillomavirus 16 E6 in anchorage-independent and invasive growth of mouse tonsil epithelium. *Arch Otolaryngol.* (2007) 133:495–502. doi: 10.1001/archotol.133.5.495
 174. Williams R, Lee DW, Elzey BD, Anderson ME, Hostager BS, Lee JH. Preclinical models of HPV+ and HPV- HNSCC in mice: an immune clearance of HPV+ HNSCC. *Head Neck.* (2009) 31:911–8. doi: 10.1002/hed.21040
 175. Mermod M, Hiou-Feige A, Bovay E, Roh V, Sponarova J, Bongiovanni M, et al. Mouse model of postsurgical primary tumor recurrence and regional lymph node metastasis progression in HPV-related head and neck cancer. *Int J Cancer.* (2018) 142:2518–28. doi: 10.1002/ijc.31240
 176. Paolini F, Massa S, Manni I, Franconi R, Venuti A. Immunotherapy in new pre-clinical models of HPV-associated oral cancers. *Hum Vaccines Immunother.* (2013) 9:534–43. doi: 10.4161/hv.23232

177. Ishida K, Tomita H, Nakashima T, Hirata A, Tanaka T, Shibata T, et al. Current mouse models of oral squamous cell carcinoma: genetic and chemically induced models. *Oral Oncol.* (2017) 73:16–20. doi: 10.1016/j.oraloncology.2017.07.028
178. Walrath JC, Hawes JJ, Van Dyke T, Reilly KM. Genetically engineered mouse models in cancer research. *Adv Cancer Res.* (2010) 106:113–64. doi: 10.1016/S0065-230X(10)06004-5
179. Lamprecht Tratar U, Horvat S, Cemazar M. Transgenic mouse models in cancer research. *Front Oncol.* (2018) 8:268. doi: 10.3389/fonc.2018.00268
180. Bian Y, Hall B, Sun ZJ, Molinolo A, Chen W, Gutkind JS, et al. Loss of TGF- β signaling and PTEN promotes head and neck squamous cell carcinoma through cellular senescence evasion and cancer-related inflammation. *Oncogene.* (2012) 31:3322–32. doi: 10.1038/onc.2011.494
181. Opitz OG, Harada H, Suliman Y, Rhoades B, Sharpless NE, Kent R, et al. A mouse model of human oral-esophageal cancer. *J Clin Invest.* (2002) 110:761–9. doi: 10.1172/JCI0215324
182. Li Z, Gonzalez CL, Wang B, Zhang Y, Mejia O, Katsonis P, et al. Cdkn2a suppresses metastasis in squamous cell carcinomas induced by the gain-of-function mutant p53(R172H). *J Pathol.* (2016) 240:224–34. doi: 10.1002/path.4770
183. Ambatipudi S, Bhosale PG, Heath E, Pandey M, Kumar G, Kane S, et al. Downregulation of keratin 76 expression during oral carcinogenesis of human, hamster and mouse. *PLoS ONE.* (2013) 8:e70688. doi: 10.1371/journal.pone.0070688
184. Chen W, Kang KL, Alshaikh A, Varma S, Lin YL, Shin KH, et al. Grainyhead-like 2 (GRHL2) knockout abolishes oral cancer development through reciprocal regulation of the MAP kinase and TGF- β signaling pathways. *Oncogenesis.* (2018) 7:38. doi: 10.1038/s41389-018-0047-5
185. Caulin C, Nguyen T, Longley MA, Zhou Z, Wang XJ, Roop DR. Inducible activation of oncogenic K-ras results in tumor formation in the oral cavity. *Cancer Res.* (2004) 64:5054–8. doi: 10.1158/0008-5472.CAN-04-1488
186. El-Bayoumy K, Chen KM, Zhang SM, Sun YW, Amin S, Stoner G, et al. Carcinogenesis of the oral cavity: environmental causes and potential prevention by black raspberry. *Chem Res Toxicol.* (2017) 30:126–44. doi: 10.1021/acs.chemrestox.6b00306
187. Frijhoff AF, Conti CJ, Senderowicz AM. Advances in molecular carcinogenesis: current and future use of mouse models to screen and validate molecularly targeted anticancer drugs. *Mol Carcinogenesis.* (2004) 39:183–94. doi: 10.1002/mc.20013
188. Munirajan AK, Mohanprasad BK, Shanmugam G, Tsuchida N. Detection of a rare point mutation at codon 59 and relatively high incidence of H-ras mutation in Indian oral cancer. *Int J Oncol.* (1998) 13:971–4. doi: 10.3892/ijo.13.5.971
189. Saranath D, Chang SE, Bhoite LT, Panchal RG, Kerr IB, Mehta AR, et al. High frequency mutation in codons 12 and 61 of H-ras oncogene in chewing tobacco-related human oral carcinoma in India. *Br J Cancer.* (1991) 63:573–8. doi: 10.1038/bjc.1991.133
190. Leemans CR, Snijders PJF, Brakenhoff RH. The molecular landscape of head and neck cancer. *Nat Rev Cancer.* (2018) 18:269–82. doi: 10.1038/nrc.2018.11
191. Ma Y, Zhang L, Huang X. Building Cre knockin rat lines using CRISPR/Cas9. *Methods Mol Biol.* (2017) 1642:37–52. doi: 10.1007/978-1-4939-7169-5_3
192. Hubbard EJ. FLP/FRT and Cre/lox recombination technology in *C. elegans*. *Methods.* (2014) 68:417–24. doi: 10.1016/j.ymeth.2014.05.007
193. Kellendonk C, Tronche F, Monaghan AP, Angrand PO, Stewart F, Schutz G. Regulation of Cre recombinase activity by the synthetic steroid RU 486. *Nucleic Acids Res.* (1996) 24:1404–11. doi: 10.1093/nar/24.8.1404
194. Chanphai P, Thomas TJ, Tajmir-Riahi HA. Design of functionalized folic acid-chitosan nanoparticles for delivery of tetracycline, doxorubicin, and tamoxifen. *J Biomol Struct Dyn.* (2019) 37:1000–6. doi: 10.1080/07391102.2018.1445559
195. Dominguez-Monedero A, Davies JA. Tamoxifen- and mifepristone-inducible versions of CRISPR effectors, Cas9 and Cpf1. *ACS Synthet Biol.* (2018) 7:2160–9. doi: 10.1021/acssynbio.8b00145
196. Nakagawa H, Inomoto T, Rustgi AK. A CACCC box-like cis-regulatory element of the Epstein-Barr virus ED-L2 promoter interacts with a novel transcriptional factor in tissue-specific squamous epithelia. *J Biol Chem.* (1997) 272:16688–99. doi: 10.1074/jbc.272.26.16688
197. Zhong R, Pytynia M, Pelizzari C, Spiotto M. Bioluminescent imaging of HPV-positive oral tumor growth and its response to image-guided radiotherapy. *Cancer Res.* (2014) 74:2073–81. doi: 10.1158/0008-5472.CAN-13-2993
198. Carper MB, Troutman S, Wagner BL, Byrd KM, Selitsky SR, Parag-Sharma K, et al. An Immunocompetent mouse model of HPV16(+) head and neck squamous cell carcinoma. *Cell Rep.* (2019) 29:1660–74.e7. doi: 10.1016/j.celrep.2019.10.005
199. Chen YF, Yang CC, Kao SY, Liu CJ, Lin SC, Chang KW. MicroRNA-211 enhances the oncogenicity of carcinogen-induced oral carcinoma by repressing TCF12 and increasing antioxidant activity. *Cancer Res.* (2016) 76:4872–86. doi: 10.1158/0008-5472.CAN-15-1664
200. Tseng SH, Yang CC, Yu EH, Chang C, Lee YS, Liu CJ, et al. K14-EGFP-miR-31 transgenic mice have high susceptibility to chemical-induced squamous cell tumorigenesis that is associating with Ku80 repression. *Int J Cancer.* (2015) 136:1263–75. doi: 10.1002/ijc.29106
201. da Silva JM, Moreira Dos Santos TP, Sobral LM, Queiroz-Junior CM, Rachid MA, Proudfoot AEI, et al. Relevance of CCL3/CCR5 axis in oral carcinogenesis. *Oncotarget.* (2017) 8:51024–36. doi: 10.18632/oncotarget.16882
202. de Oliveira Santos D, Loyola AM, Cardoso SV, Chammas R, Liu FT, de Faria PR. Hedgehog signaling pathway mediates tongue tumorigenesis in wild-type mice but not in Gal3-deficient mice. *Exp Mol Pathol.* (2014) 97:332–7. doi: 10.1016/j.yexmp.2014.09.018
203. da Silva JM, Dos Santos TPM, Saraiva AM, Fernandes de Oliveira AL, Garlet GP, Batista AC, et al. Role of atypical chemokine receptor ACKR2 in experimental oral squamous cell carcinogenesis. *Cytokine.* (2019) 118:160–7. doi: 10.1016/j.cyto.2018.03.001

Conflict of Interest: The authors declare that the research was conducted in the absence of any commercial or financial relationships that could be construed as a potential conflict of interest.

Copyright © 2020 Li, Dong, Yang, Song, Mou and Ni. This is an open-access article distributed under the terms of the Creative Commons Attribution License (CC BY). The use, distribution or reproduction in other forums is permitted, provided the original author(s) and the copyright owner(s) are credited and that the original publication in this journal is cited, in accordance with accepted academic practice. No use, distribution or reproduction is permitted which does not comply with these terms.